Sandia National Laboratories

SAND2019-4829C

High-fidelity quantum operations in microfabricated surface ion traps

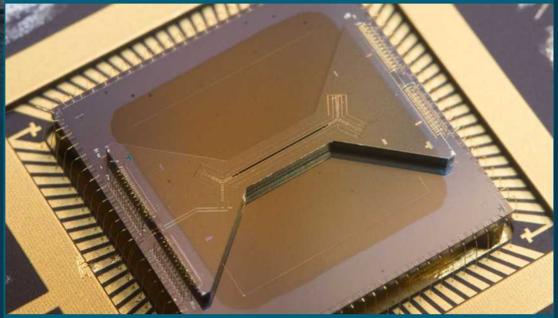

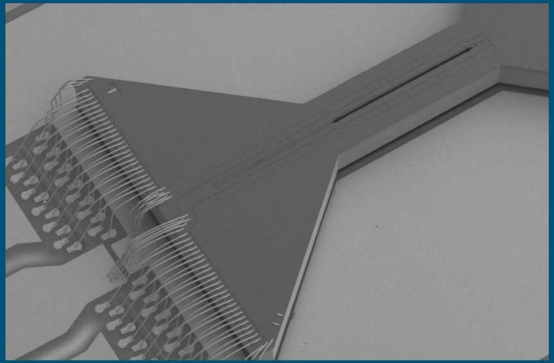

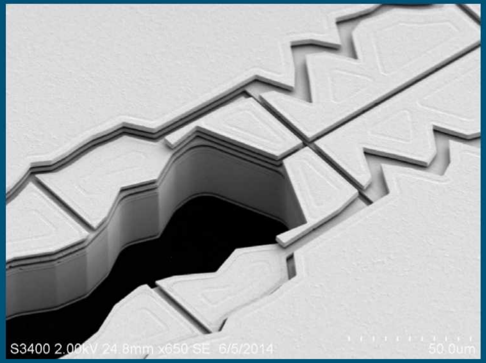

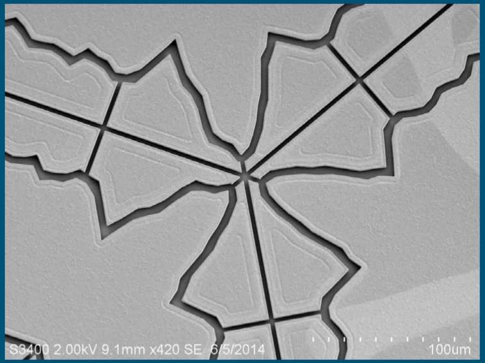

U.S. DEPARTMENT OF ENERGY
Office of Science

IARPA
BE THE FUTURE

PRESENTED BY

Peter Maunz

U.S. DEPARTMENT OF ENERGY NNSA National Nuclear Security Administration

Sandia National Laboratories is a multimission laboratory managed and operated by National Technology & Engineering Solutions of Sandia, LLC, a wholly owned subsidiary of Honeywell International Inc., for the U.S. Department of Energy's National Nuclear Security Administration under contract DE-NA0003525.

Why microfabrication

- Microfabrication enables scalable traps
  - Junctions and transitions
  - Integration of passive and active components
  - Integration of optics
- Repeatable and reproducible properties
  - Fabrication of identical devices

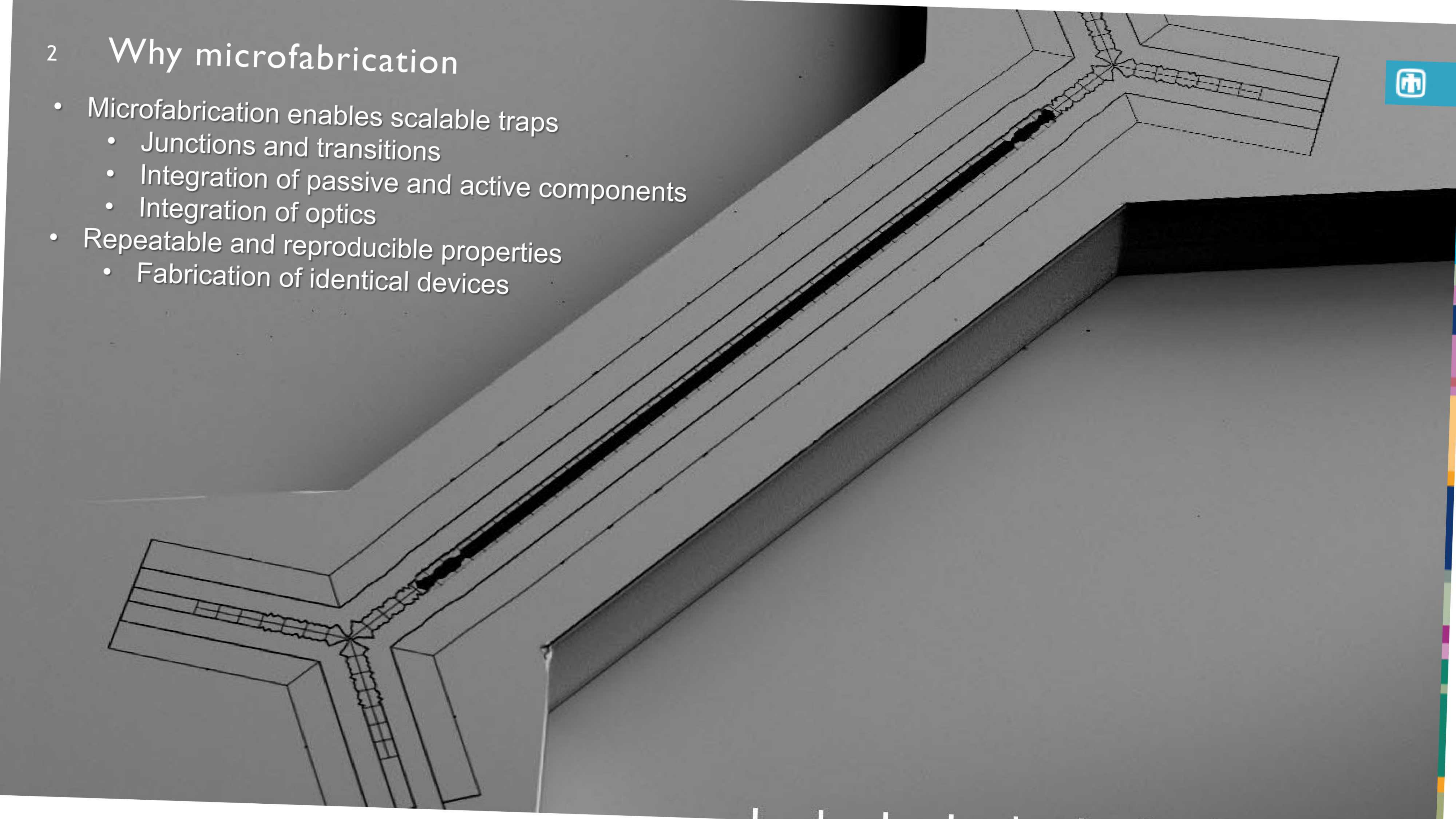

Challenges of microfabrication

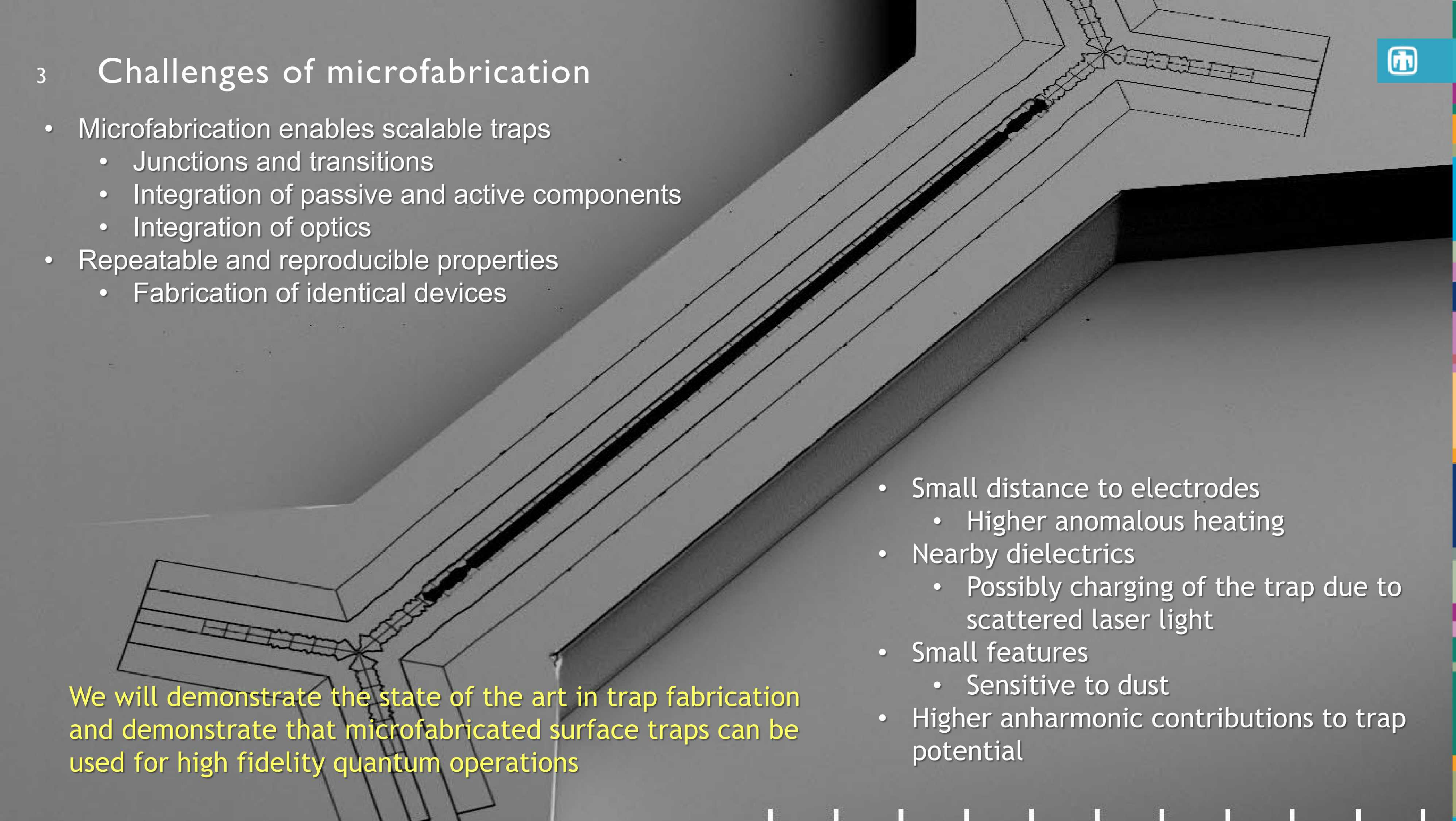

- Microfabrication enables scalable traps
  - Junctions and transitions
  - Integration of passive and active components
  - Integration of optics
- Repeatable and reproducible properties
  - Fabrication of identical devices

- Small distance to electrodes
  - Higher anomalous heating
- Nearby dielectrics
  - Possibly charging of the trap due to scattered laser light
- Small features
  - Sensitive to dust
- Higher anharmonic contributions to trap potential

We will demonstrate the state of the art in trap fabrication and demonstrate that microfabricated surface traps can be used for high fidelity quantum operations

Outline

Trap fabrication capabilities

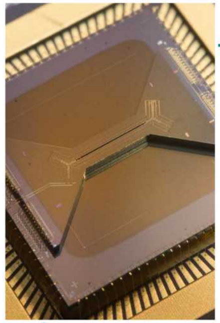

Sandia's High-Optical-Access (HOA) trap

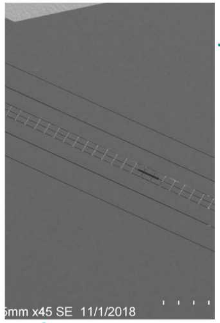

Phoenix trap

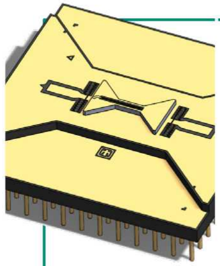

Custom trap package

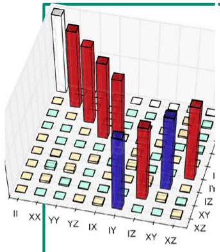

Quantum operations in surface traps

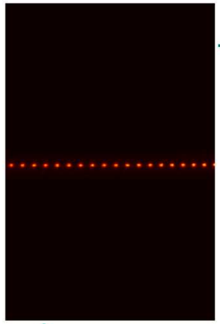

QSCOUT quantum testbed

Trap fabrication capabilities

- Based on CEMOS back of line
- Crucial capabilities outside CMOS integrated
- Up to 6-level metallization
  - Planarized
  - Islanded electrodes
  - Reduced rf capacitance
  - Any electrode geometry can be realized
- Removed dielectric (better shielding)
- Integrated trench capacitors for rf shunting
- Loading holes and slots
- Release singulation (e.g. bowtie shapes)

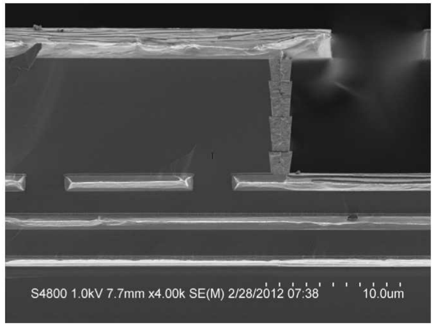

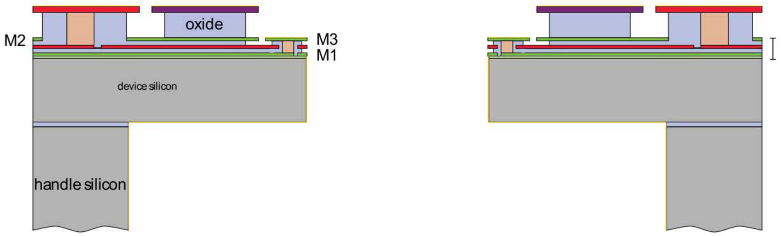

Switchable Y Junction

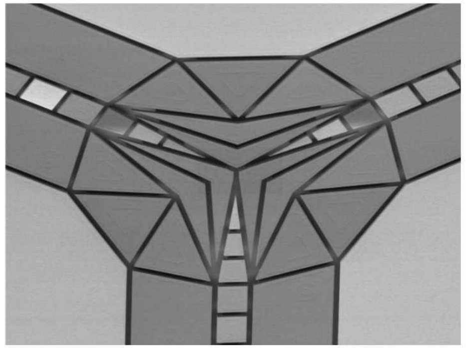

Ring Trap

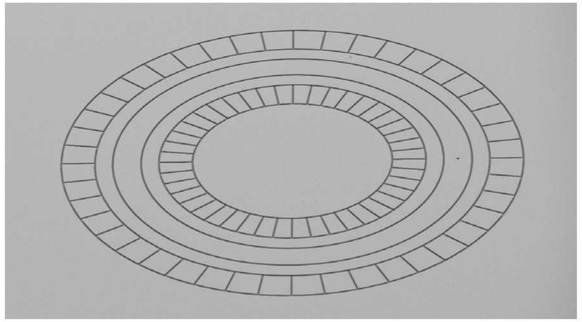

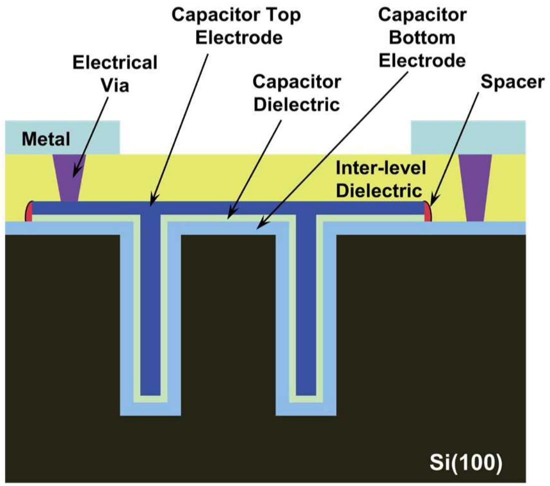

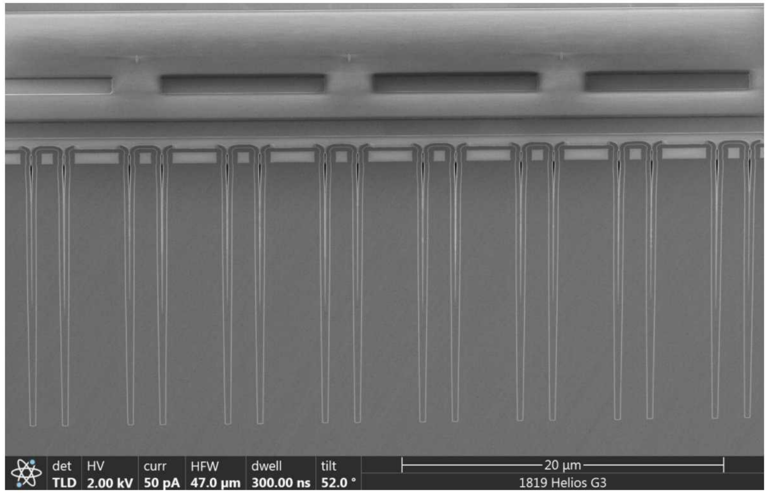

High Optical Access trap HOA-2

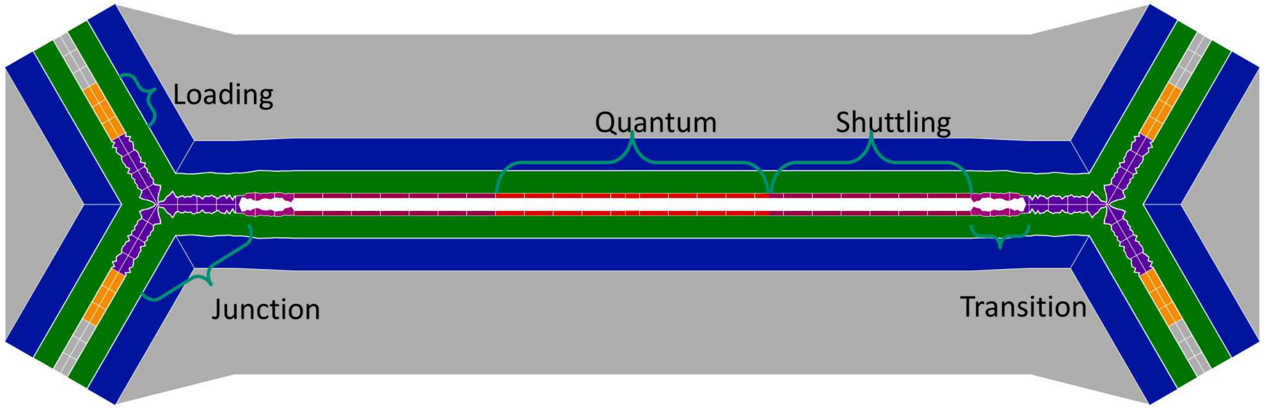

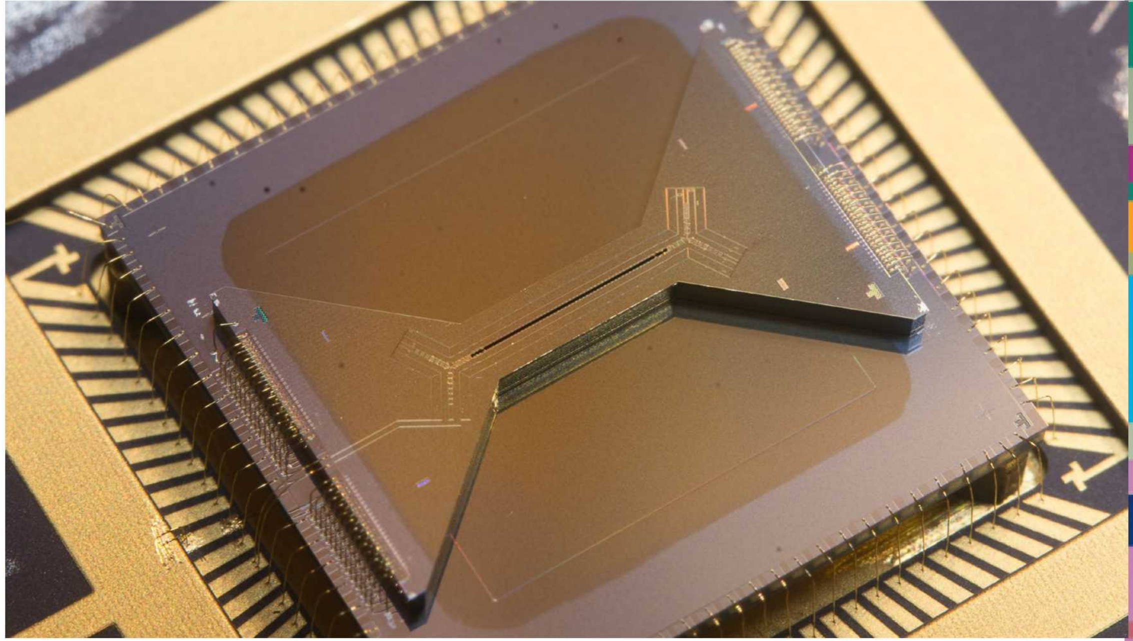

- Excellent optical access rivaling 3-D
  - 2π for imaging
  - NA=0.2 through slot
  - NA=0.12 skimming surface
- High trap frequencies (characteristic distance 140µm)
- Full control over principal axes orientation
- Junctions
- Transitions between slotted and above-surface trap regions

Ytterbium trap characteristics

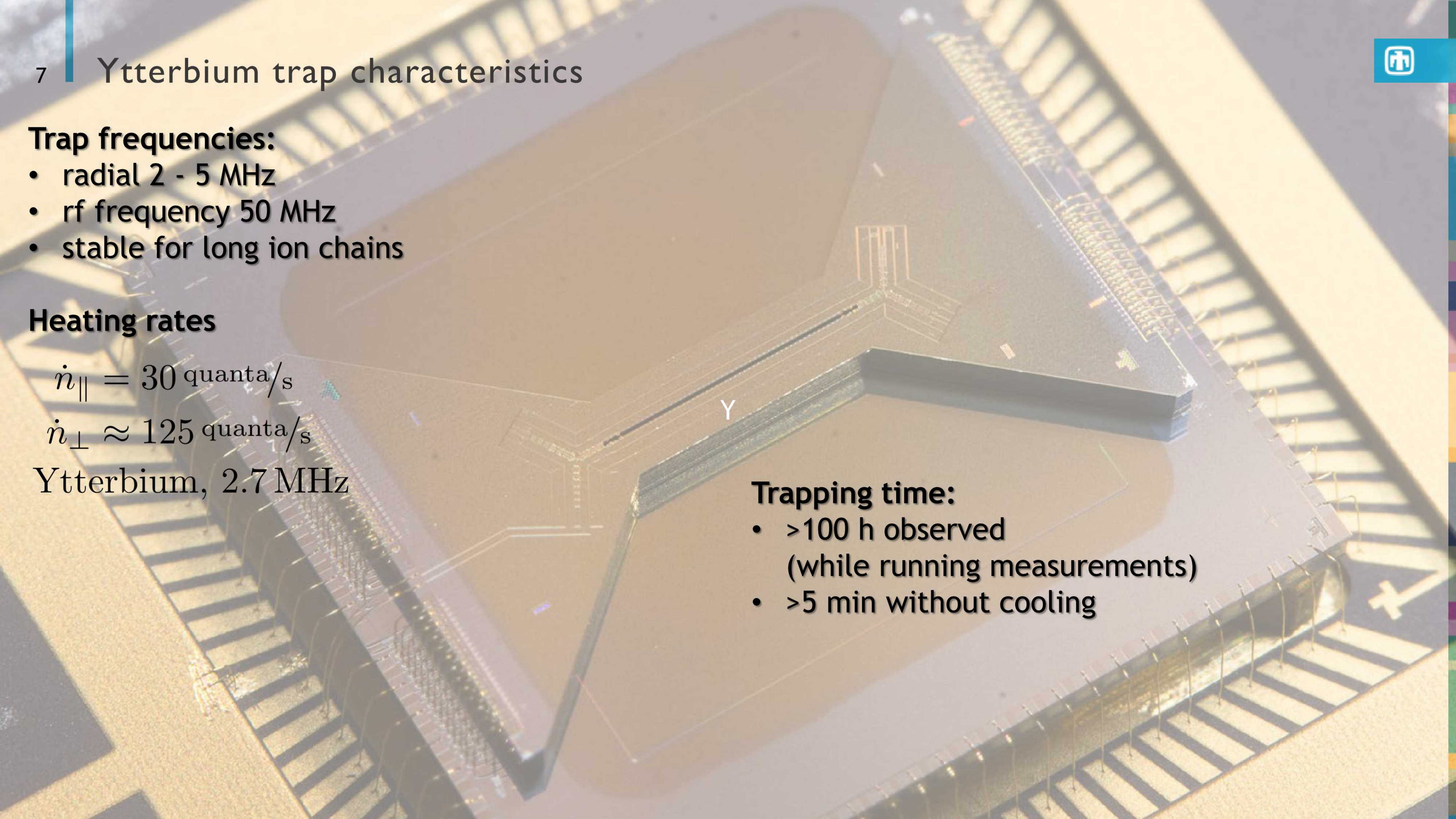

Trap frequencies:

- radial 2 - 5 MHz
- rf frequency 50 MHz
- stable for long ion chains

Heating rates

$$\dot{n}_{\parallel} = 30\,\mathrm{quanta/s}$$

$$\dot{n}_{\perp} \approx 125\,\mathrm{quanta/s}$$

$$\mathrm{Ytterbium},\ 2.7\,\mathrm{MHz}$$

Trapping time:

- >100 h observed
  (while running measurements)
- >5 min without cooling

Calculating voltage solutions

- Boundary element simulation for surface electrode geometry

$$\mathcal{H} = \begin{pmatrix} \frac{\partial\phi}{\partial x\partial x} & \frac{\partial\phi}{\partial x\partial y} & \frac{\partial\phi}{\partial x\partial z} \\ \frac{\partial\phi}{\partial y\partial x} & \frac{\partial\phi}{\partial y\partial y} & \frac{\partial\phi}{\partial y\partial z} \\ \frac{\partial\phi}{\partial z\partial x} & \frac{\partial\phi}{\partial z\partial y} & \frac{\partial\phi}{\partial z\partial z} \end{pmatrix}$$

- Symmetric curvature tensor
- 6 degrees of freedom
- Determines trap frequencies and principal axes rotations
- Traceless for static fields
- Trace is generated by rf pseudopotential

- Calculate voltage solutions to independently control curvature tensor elements and fields at ion locations
- Use pseudo-inverse to get well-defined solution using nearby electrodes with minimal voltages
- Generate solution for any trap configuration from these basis-solutions

Advantages of parametric trapping solutions:
- Primitives are in terms of curvature tensor elements and can be applied at any location in the trap.
- Shuttling primitives can be easily combined

Example:
- Rotating ion crystal while translating through the trap

Principal axes rotation

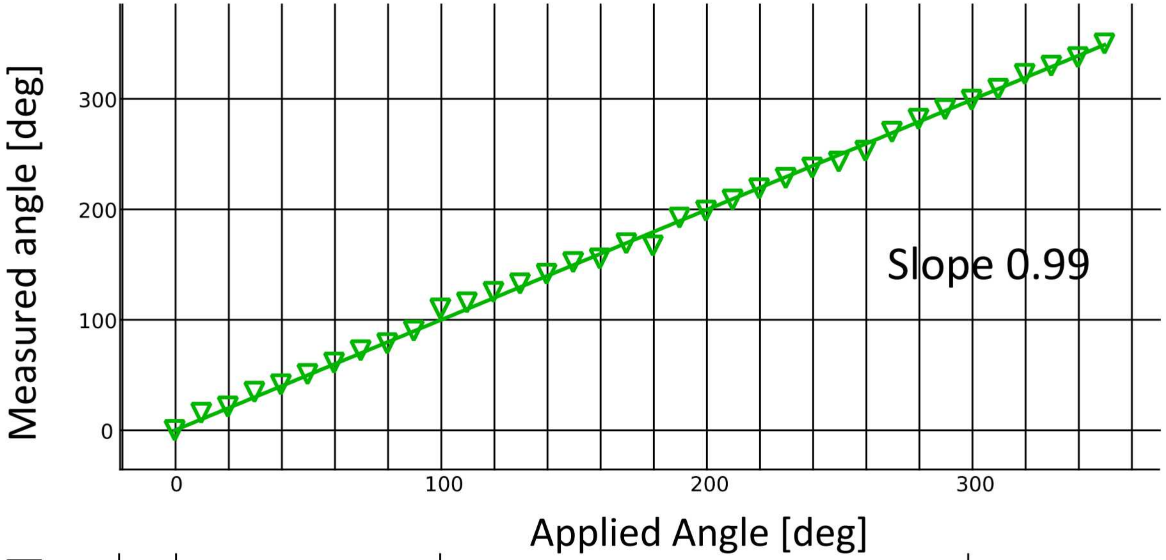

- Do we understand the trapping fields?
- Principal axes rotation realized as in simulation
- No change in trap frequencies

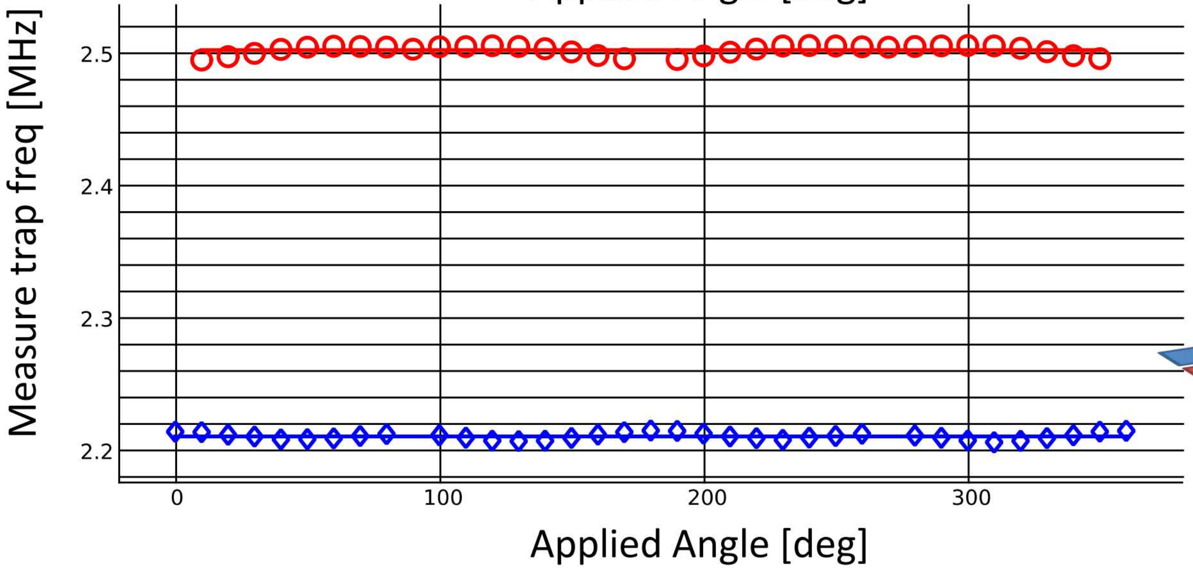

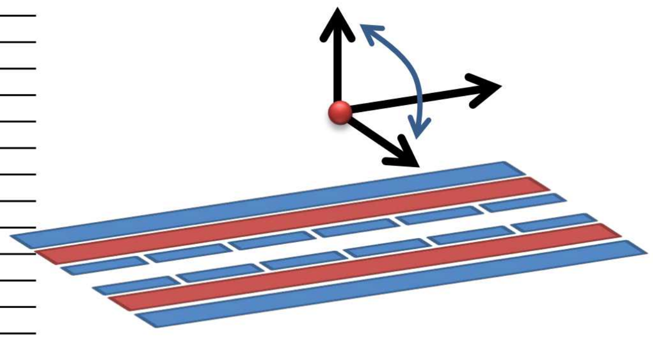

The simulations accurately describe the fields and curvatures generated by the trap

Rotation of ion chains

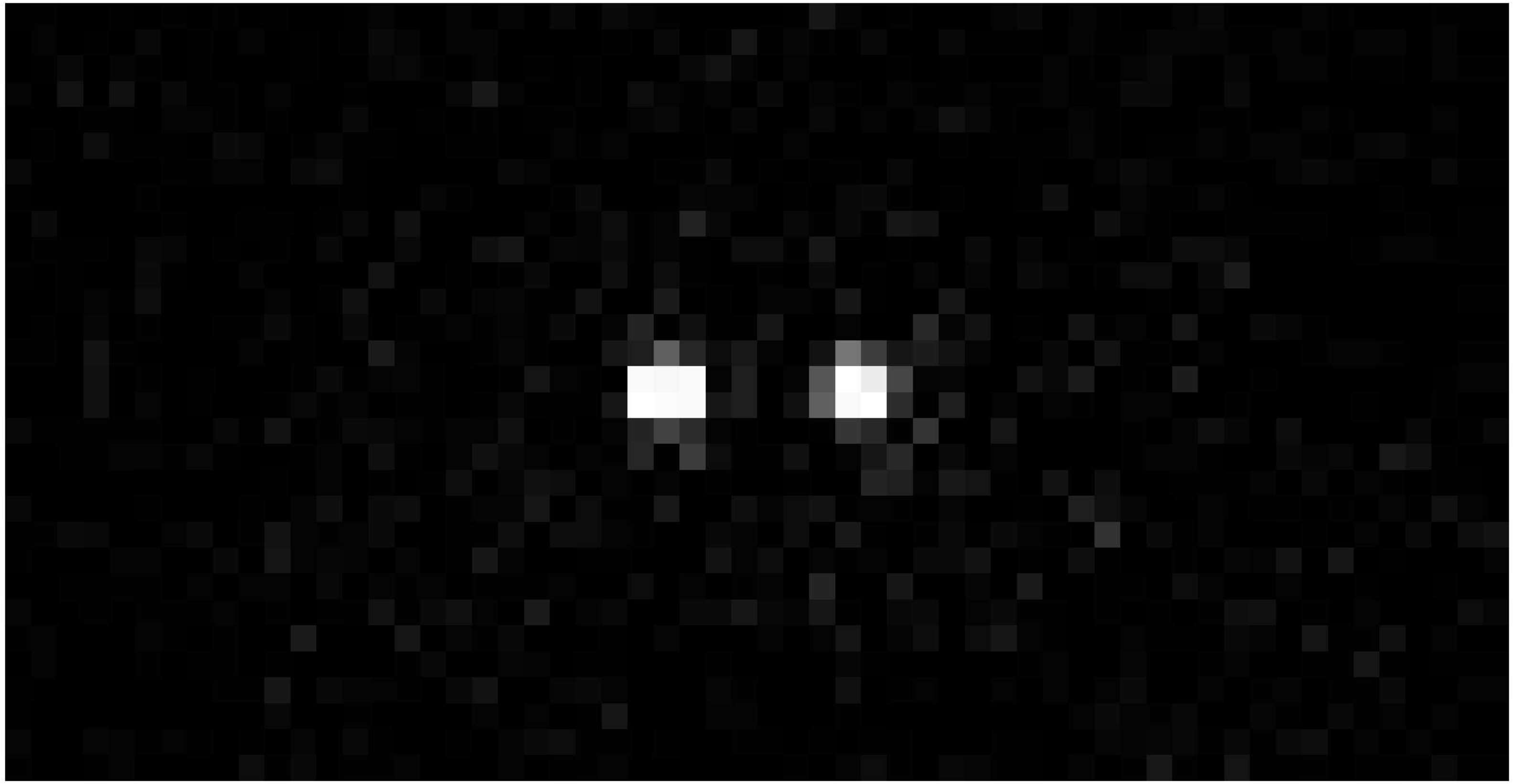

To be characterized as function of swapping time

- Swapping fidelity
- Accumulated motion

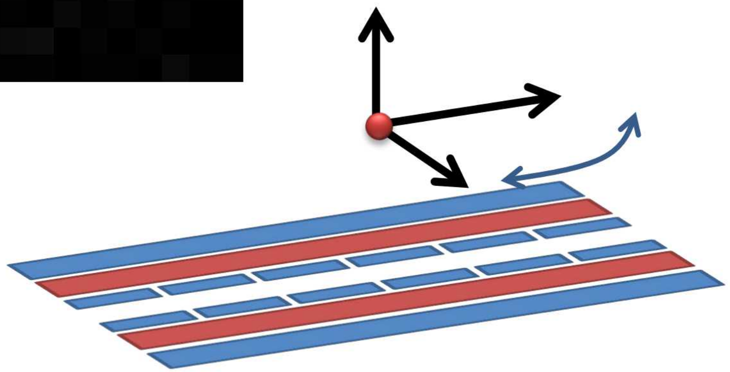

Measuring swap fidelity

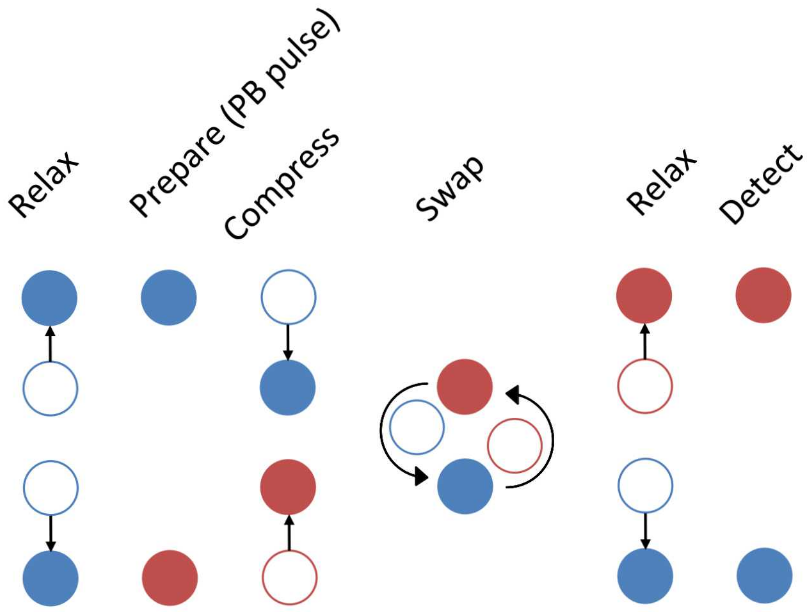

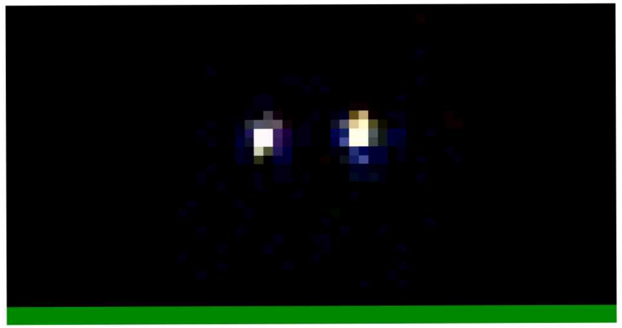

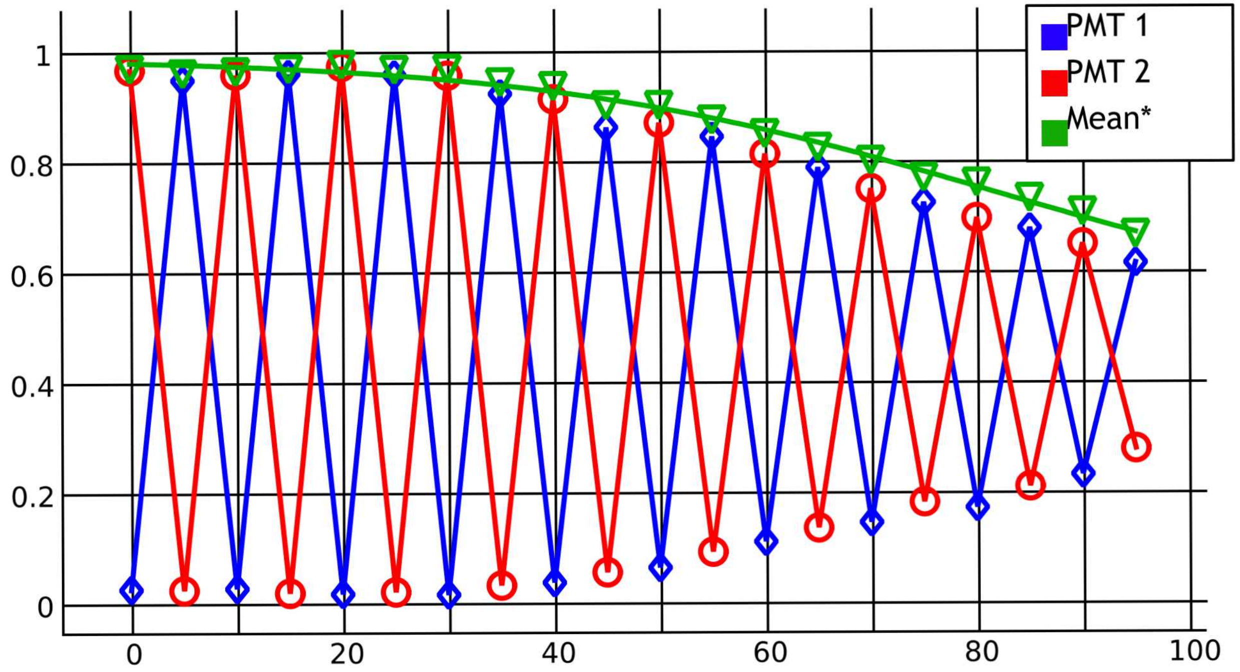

Separation and merging of ions

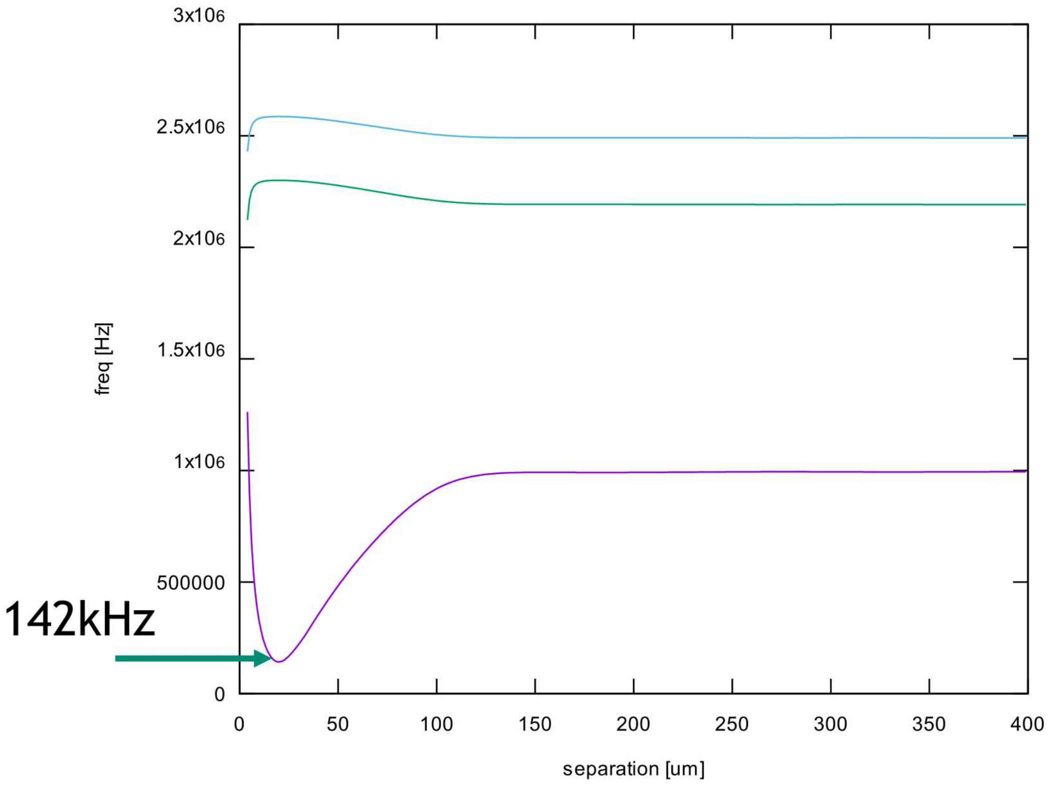

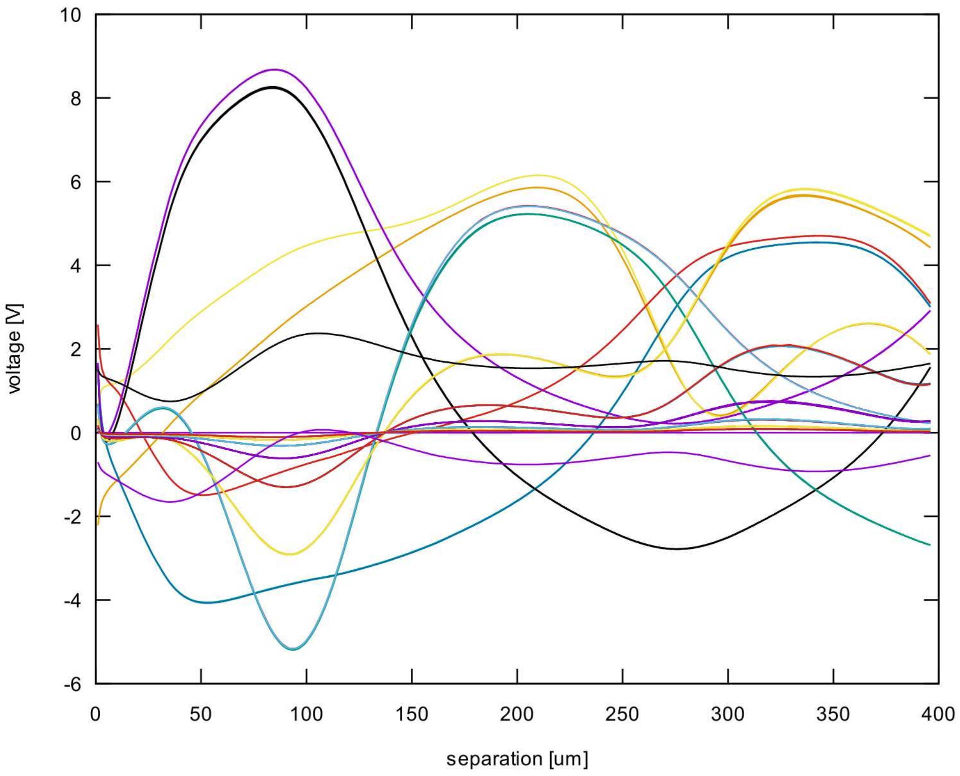

RF dissipation

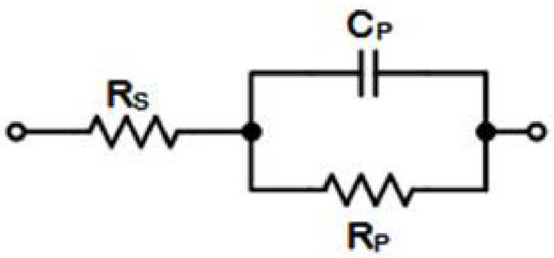

$$P_s \approx \frac{1}{2} R_s U^2 \omega^2 C_p^2$$

$$P_p = \frac{1}{2} \frac{\omega U^2}{R_p}$$

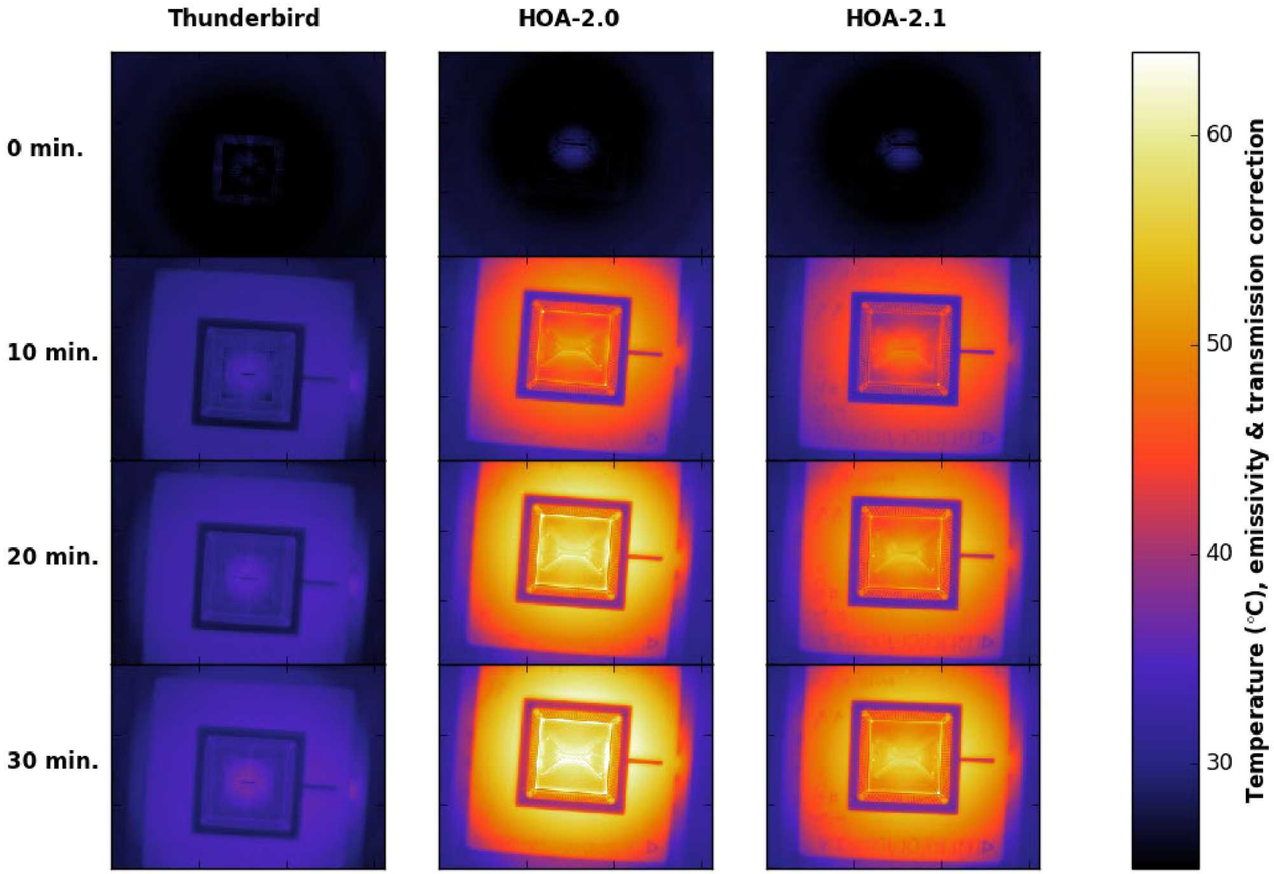

RF Voltage at trap (~280 V)

For 100 V amplitude at 100 MHz:

Trap	Temp	C_p	R_s	R_p	P_s	P_p
HOA-2	300 K	7.6 pF	1.2 Ω	1.2 MΩ	140 mW	4.2 mW
	4 K		0.5 Ω		60 mW	
HOA-2.1	300 K	7.6 pF	0.9 Ω	1.6 MΩ	100 mW	3.1 mW
	4 K		0.5 Ω		60 mW	
Thunderbird	300 K	2.4 pF	0.6 Ω	1.5 MΩ	6.7 mW	3.3 mW

Sandia Traps

Y-junction traps

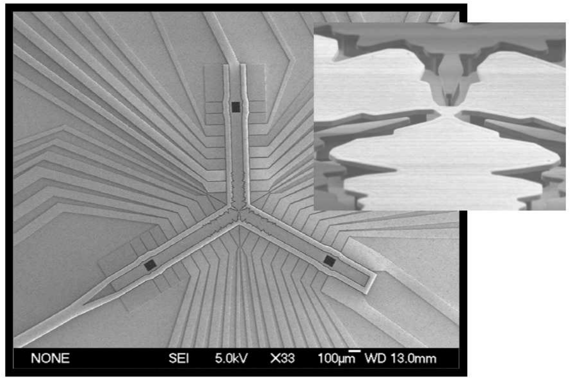

Circulator trap

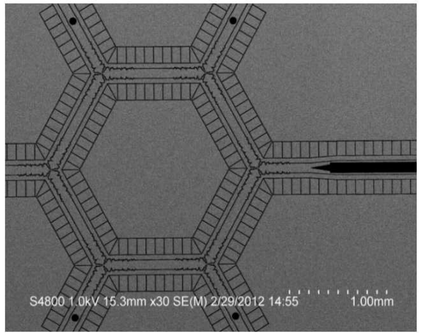

High Optical Access (HOA) trap

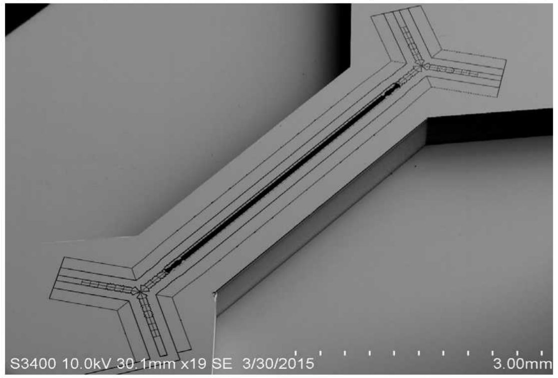

Ring trap:

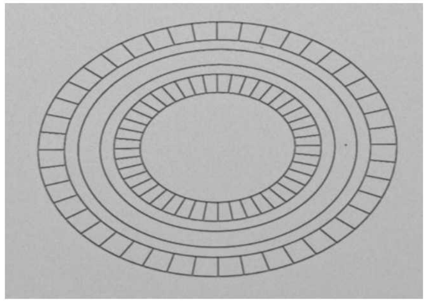

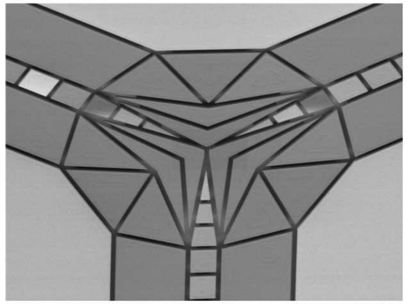

Switchable RF junction trap

Stylus trap

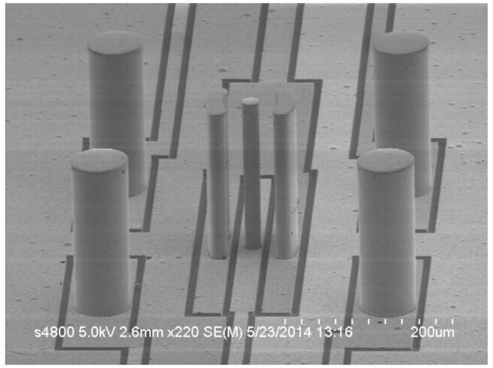

Microwave trap

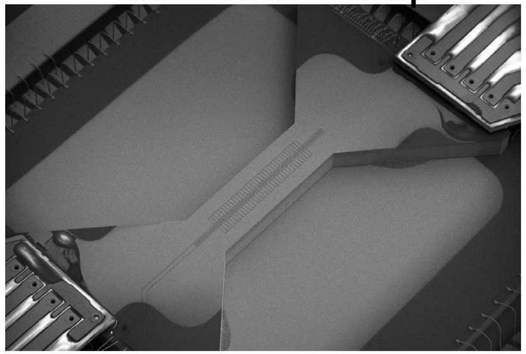

EPICS trap

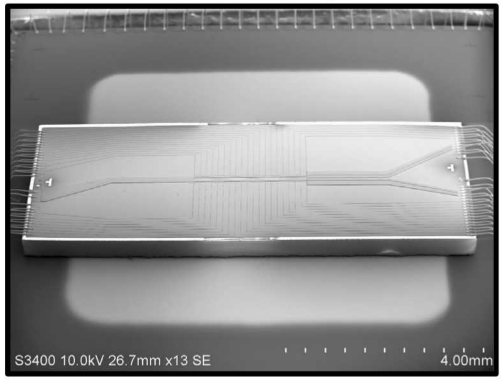

Phoenix trap fabrication
Original plans for Phoenix

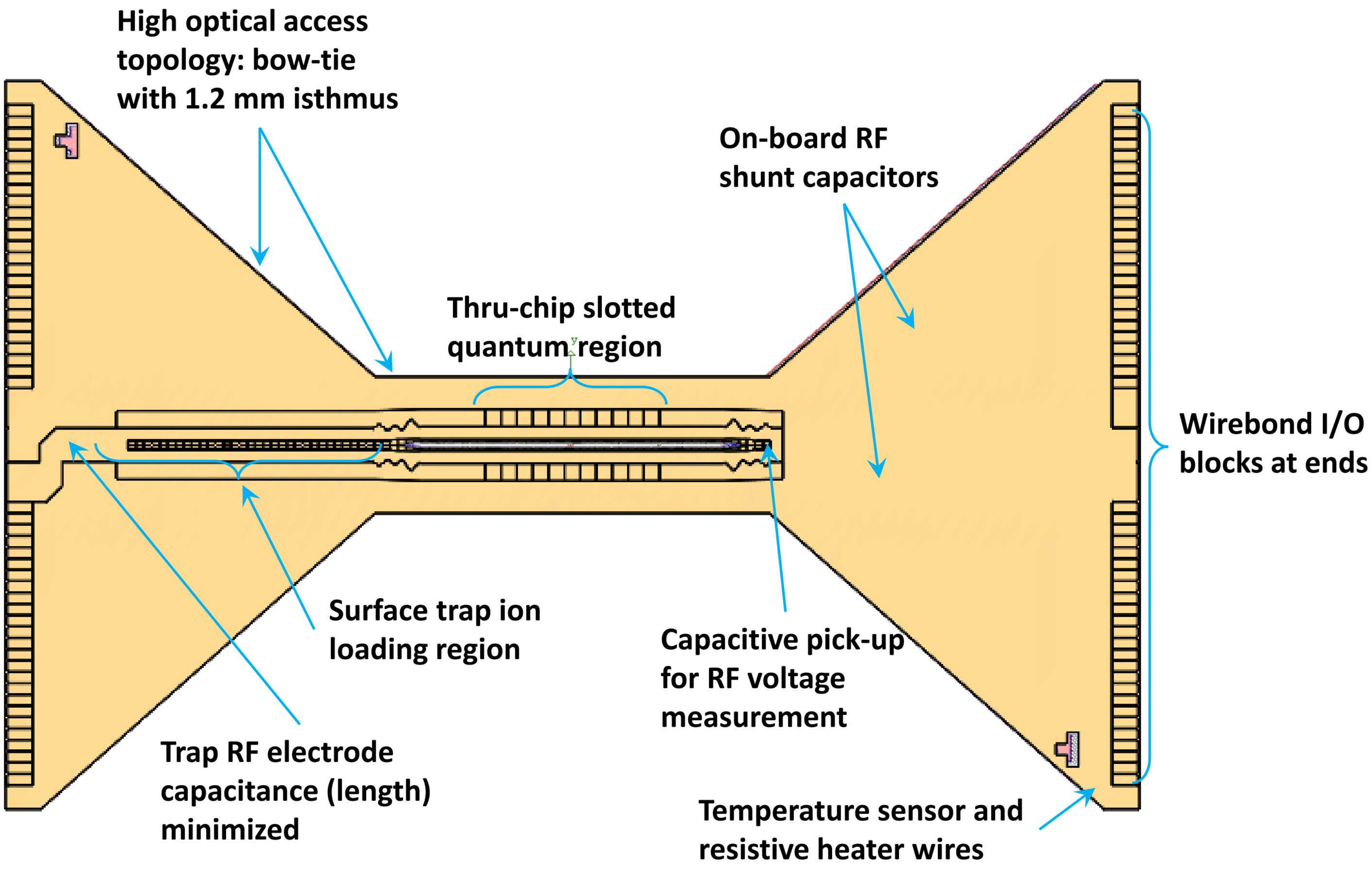

Phoenix trap fabrication
Trap features

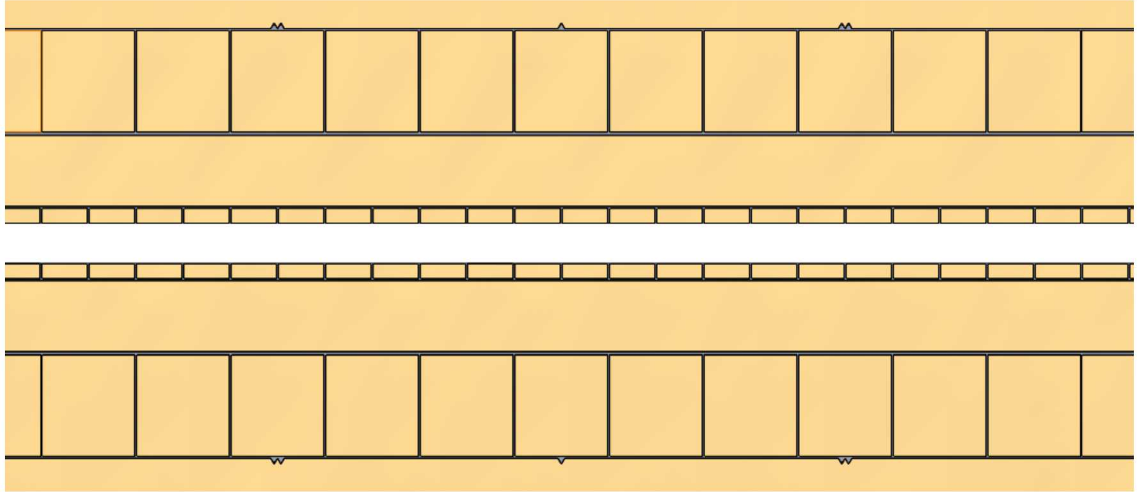

<u>Quantum region</u>

- Segmentation of 22 inner electrode pairs and 11 outer pairs for better control of ion chains and spatial re-ordering of ions
- 22×70µm = 1540µm long
- Ion height 70µm

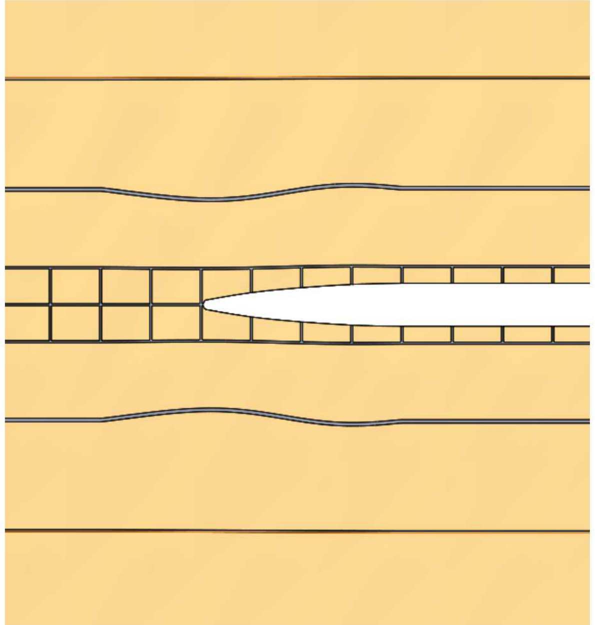

<u>Transition</u>

- 9 degrees of freedom
- Low spatial frequencies

<u>Loading region</u>

- 5 electrode pairs
- Loading slot 180um x 3um

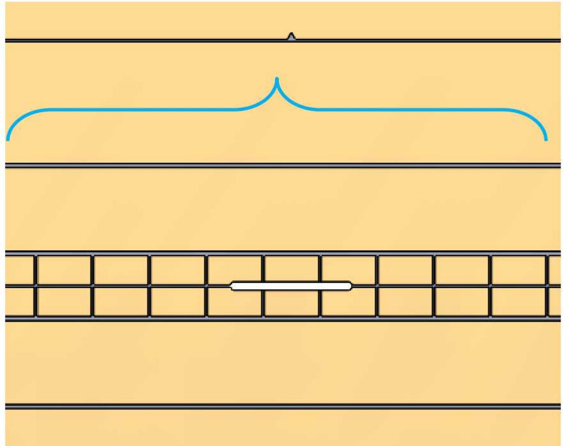

Phoenix trap
Transition characterization

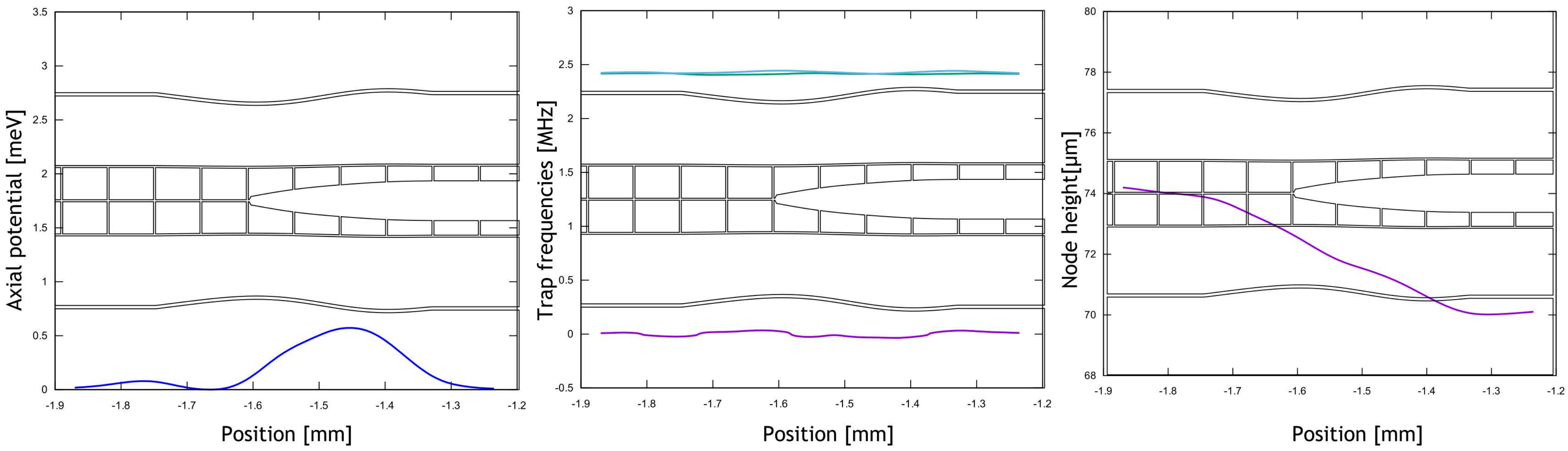

- Transition between slotted and above surface parts of trap is optimized to minimize variations in the trace of the curvature tensor
- RF pseudopotential hump is about 0.5meV for a 2.5MHz radial trap frequency
- Ion height above slot and above surface differs to keep trap frequencies (trace of curvature tensor) constant

Rf-dissipation in traps
electrical characterization

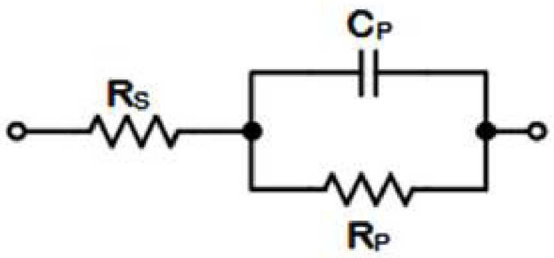

R_s : Series resistance (lead resistance)

R_p : (rf) parallel resistance (dielectric absorption)

C_p : capacitance

For 100 V amplitude at 100 MHz:

Trap	Temp	C_p	R_s	R_p	P_s	P_p
Phoenix-0 (measurement)	300 K	4 pF	0.4 Ω		5 mW	
Phoneix-surface (calc.)	4 K		0.05 Ω		1 mW	
Phoenix-slotted (calc.)	300 K	5.5 pF	0.4 Ω		9.4 mW	
	4 K		0.05 Ω		1.4 mW	
HOA-2.1	300 K	7.6 pF	0.9 Ω	1.6 MΩ	100 mW	3.1 mW
	4 K		0.5 Ω		60 mW	
Thunderbird	300 K	2.4 pF	0.6 Ω	1.5 MΩ	6.7 mW	3.3 mW

$$P_s \approx \frac{1}{2} R_s U^2 \omega^2 C_p^2$$

$$P_p = \frac{1}{2} \frac{\omega U^2}{R_p}$$

Custom trap package

Legacy 4 Level CPGA Packaging Assembly

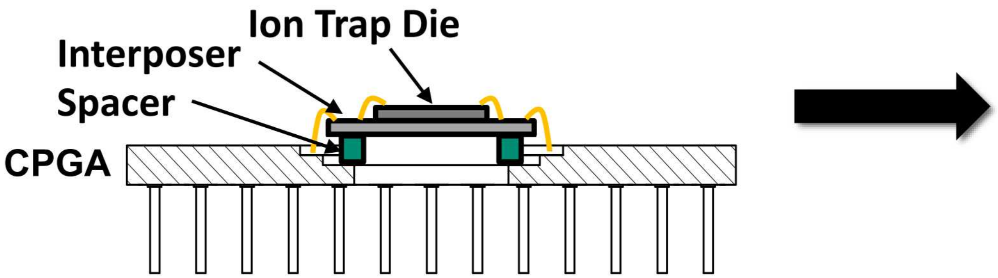

Simplified 2 part assembly

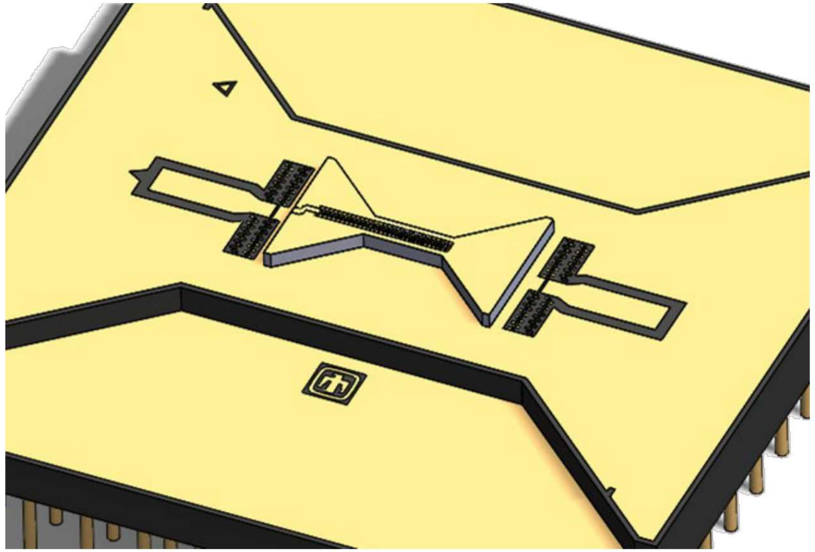

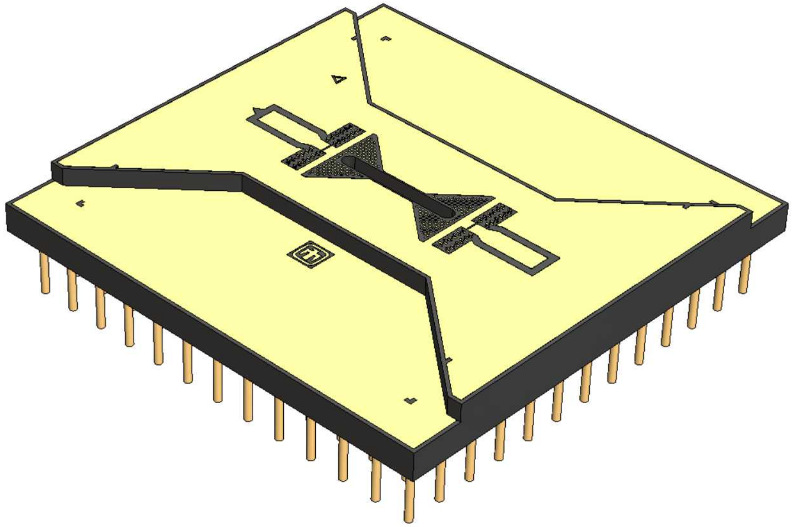

Objectives:

- Improved rf- and ground performance
- Compatible with bowtie chip without interposer
- Simplified assembly
- Backwards compatibility with MQCO package

Properties:

- AlN for improved thermal conductivity and reduced thermal expansion vs Al_2O_3
- Two rf connections with minimized capacitance (3pF) and resistivity (50mOhm)
- Backwards compatible with prior HOA devices
- Metal coverage of top surface
- All metal is signal or ground (no floating metals)

Custom trap package Is available

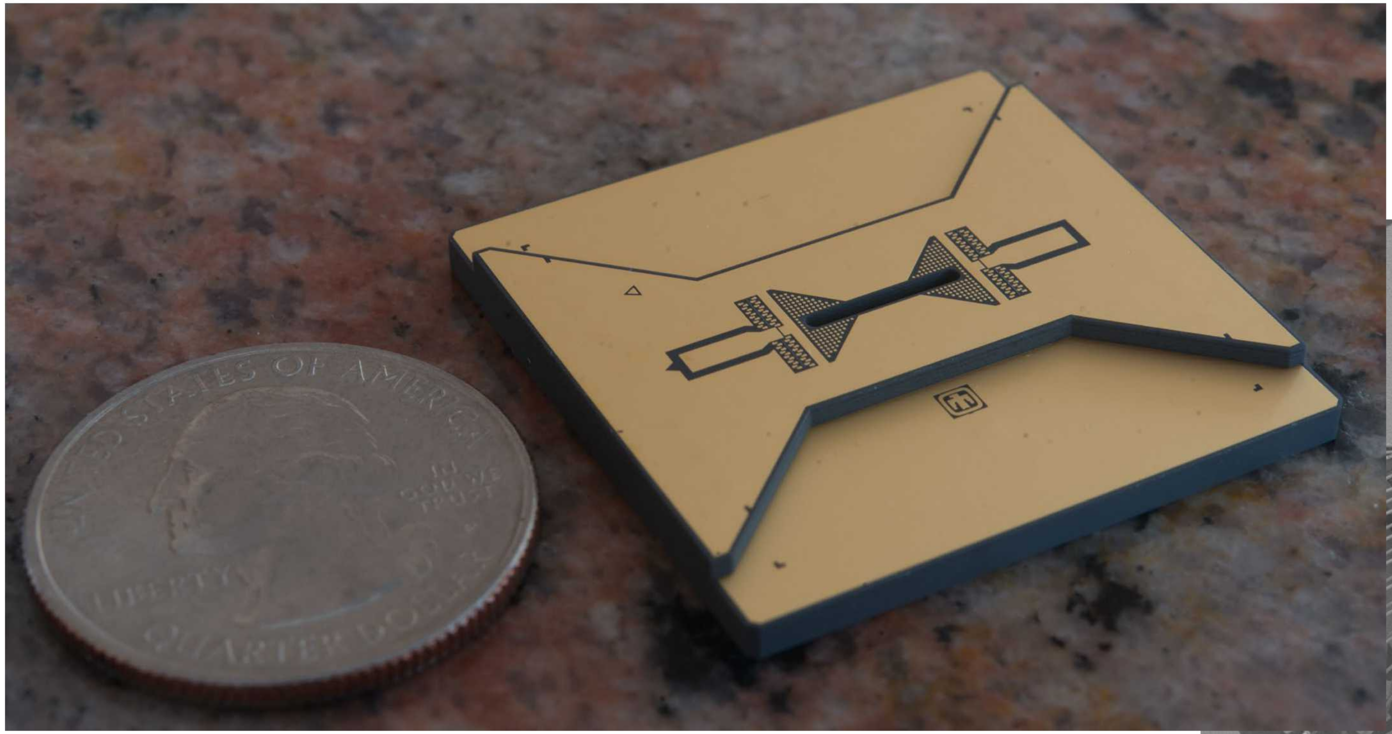

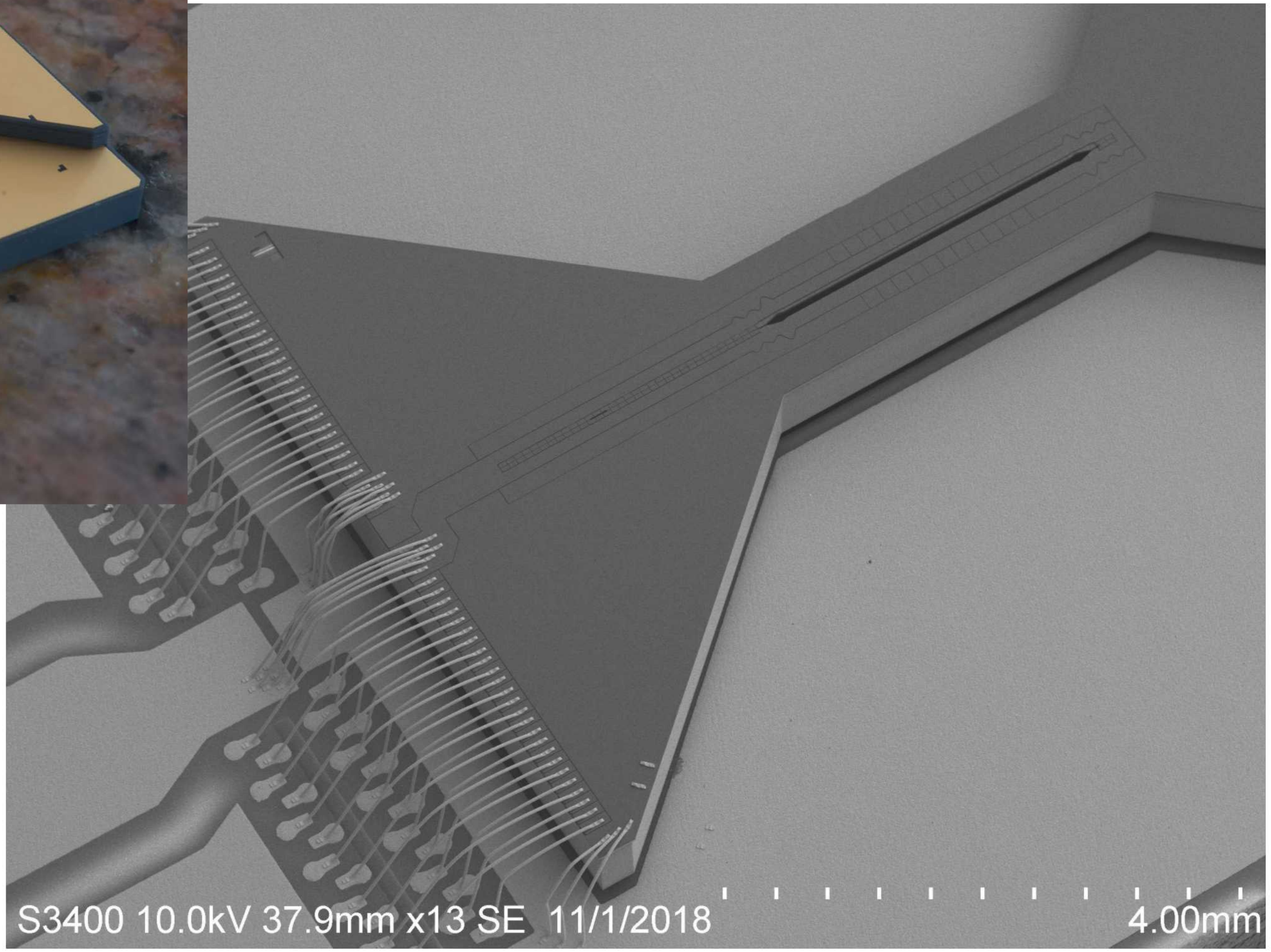

Compared to commercial off the shelf package

- Top surface mostly metal (grounded)
- Low resistance of rf and ground paths (massively parallel vias, routing on outer layers)

Gate Set Tomography (GST)

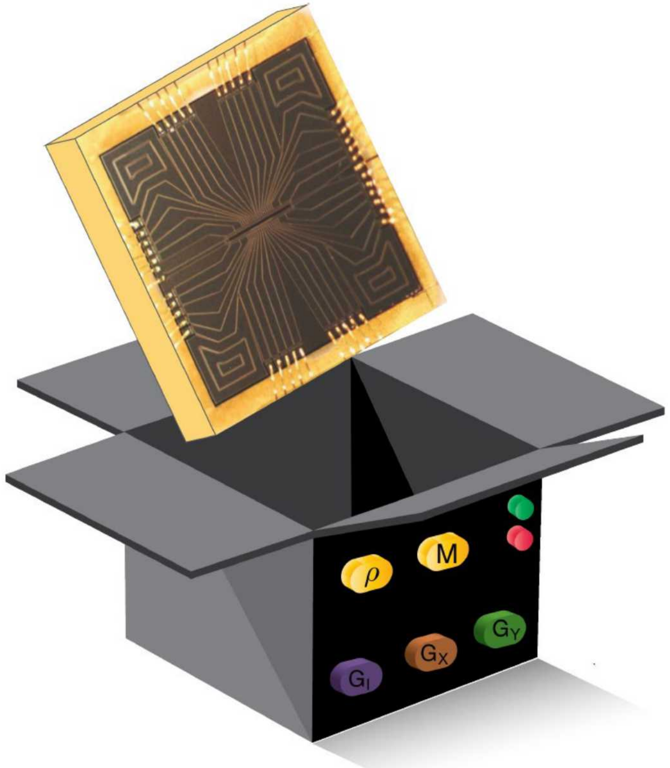

Developed at Sandia by QCVV team

- No calibration required
- Detailed debug information
- Efficiently measures performance characterizing fault-tolerance (diamond norm)
- Detects non-Markovian noise

Uses structured sequences to amplify all possible errors

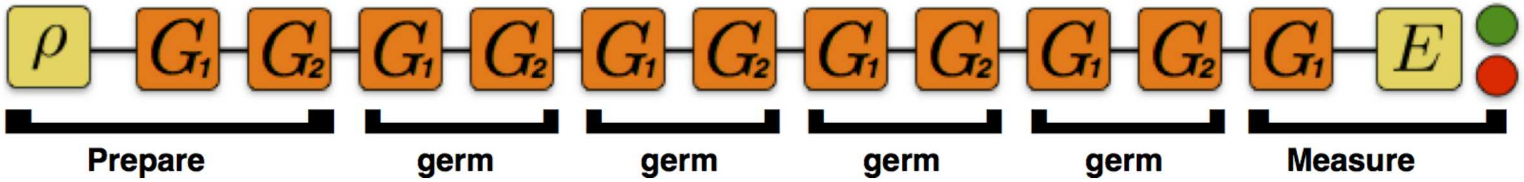

GST sequences

Single qubit BB1 compensated microwave gates on $^{171}Yb^{+}$

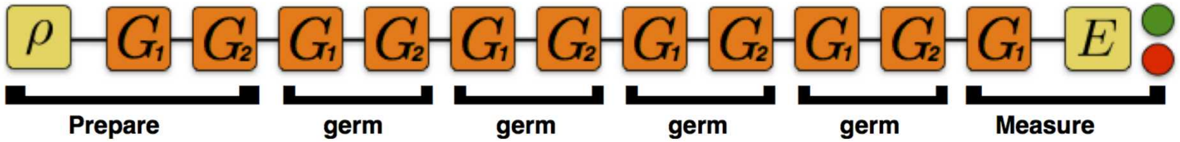

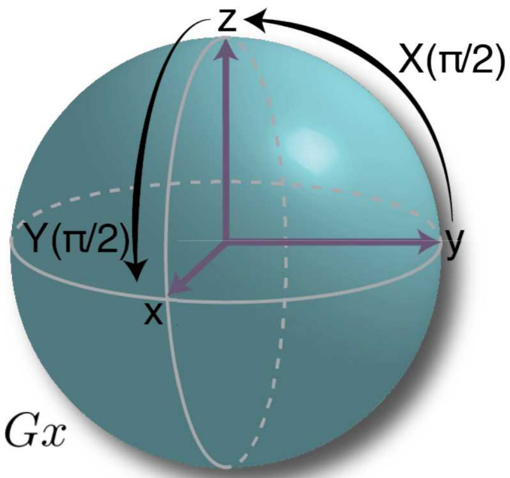

Desired "target" gates:

G_i	Idle (Identity)
G_x	$\pi/2$ rotation about x-axis
G_y	$\pi/2$ rotation about y-axis

Fiducials:

$\{\}$

Gx

Gy

$Gx \cdot Gx$

$Gx \cdot Gx \cdot Gx$

$Gy \cdot Gy \cdot Gy$

Approximately prepare 6 points on Bloch sphere

Germs:

Gx

Gy

Gi

$Gx \cdot Gy$

$Gx \cdot Gy \cdot Gi$

$Gx \cdot Gi \cdot Gy$

$Gx \cdot Gi \cdot Gi$

$Gy \cdot Gi \cdot Gi$

$Gx \cdot Gx \cdot Gi \cdot Gy$

$Gx \cdot Gy \cdot Gy \cdot Gi$

$Gx \cdot Gx \cdot Gy \cdot Gx \cdot Gy \cdot Gy$

GST: debugging microwave gates

Gate	Rotn. axis	Angle
G_I	0.5252 -0.009 0.8506 -0.0244	0.001699π
G_X	-3×10^{-6} -1 -3×10^{-5} -0.009	0.501308π
G_Y	-0.2474 0.0001 0.9689 -0.0001	0.501366π

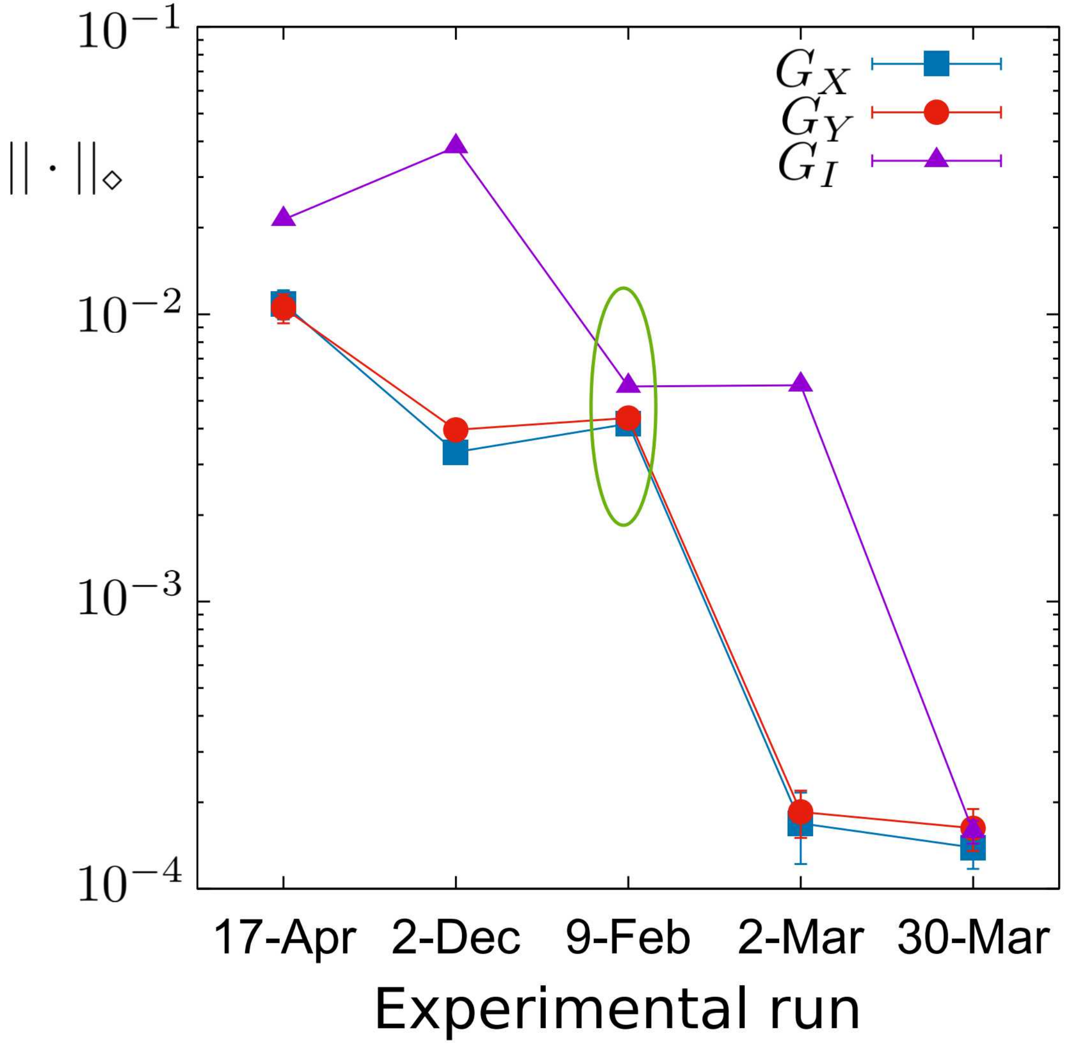

GST: debugging microwave gates

Gate	Rotn. axis	Angle
G_I	0.5252 -0.009 0.8506 -0.0244	0.001699π
G_X	-3×10^{-6} -1 -3×10^{-5} -0.009	0.501308π
G_Y	-0.2474 0.0001 0.9689 -0.0001	0.501366π

Gate	Rotn. axis	Angle
G_I	-0.0035 0.014 -0.9999 0.0006	0.001769π
G_X	-3×10^{-5} -1 1×10^{-4} 0.0006	0.500007π
G_Y	0.1104 4×10^{-5} 0.9939 0.0005	0.50001π

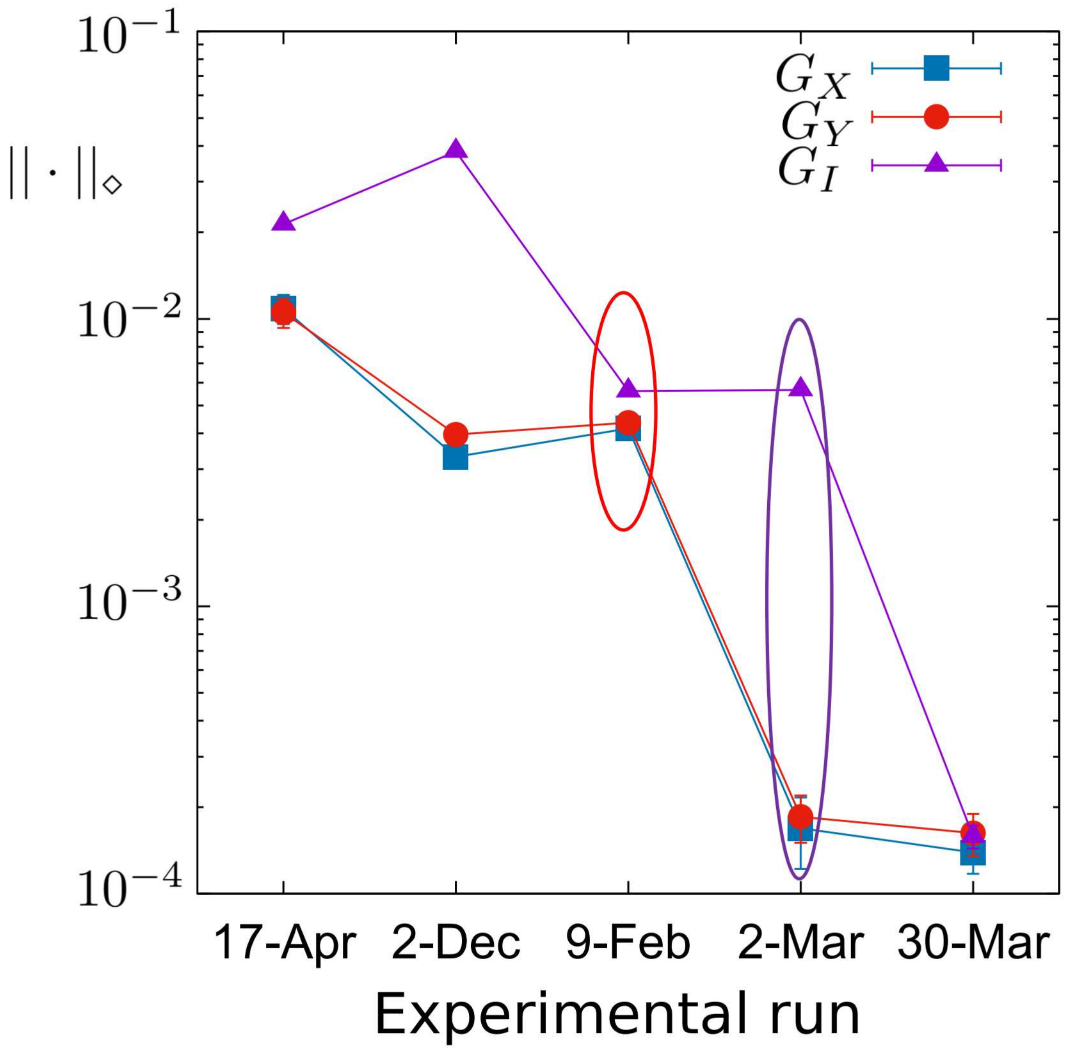

Context and time dependency of gates

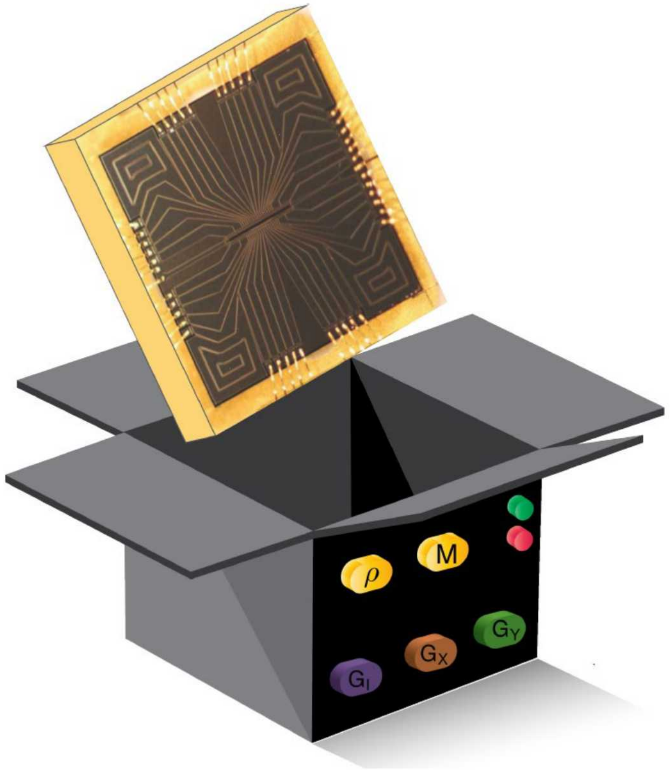

Assumptions:

- Qubits in a box
- Pressing a button always executes the exactly same operation
- Independent from context (gates executed before)
- Independent from when a gate is executed

GST uses a large (over-complete) number of sequences.

We can look whether the assumptions are satisfied

Ongoing work to improve and distinguish detection of context and time dependence of classical control

GST model violation

The χ^2 values from the fits are expected to follow a χ^2 distribution with mean k and standard deviation $\sqrt{2k}$

$$\frac{\chi^2 - k}{\sqrt{2k}}$$

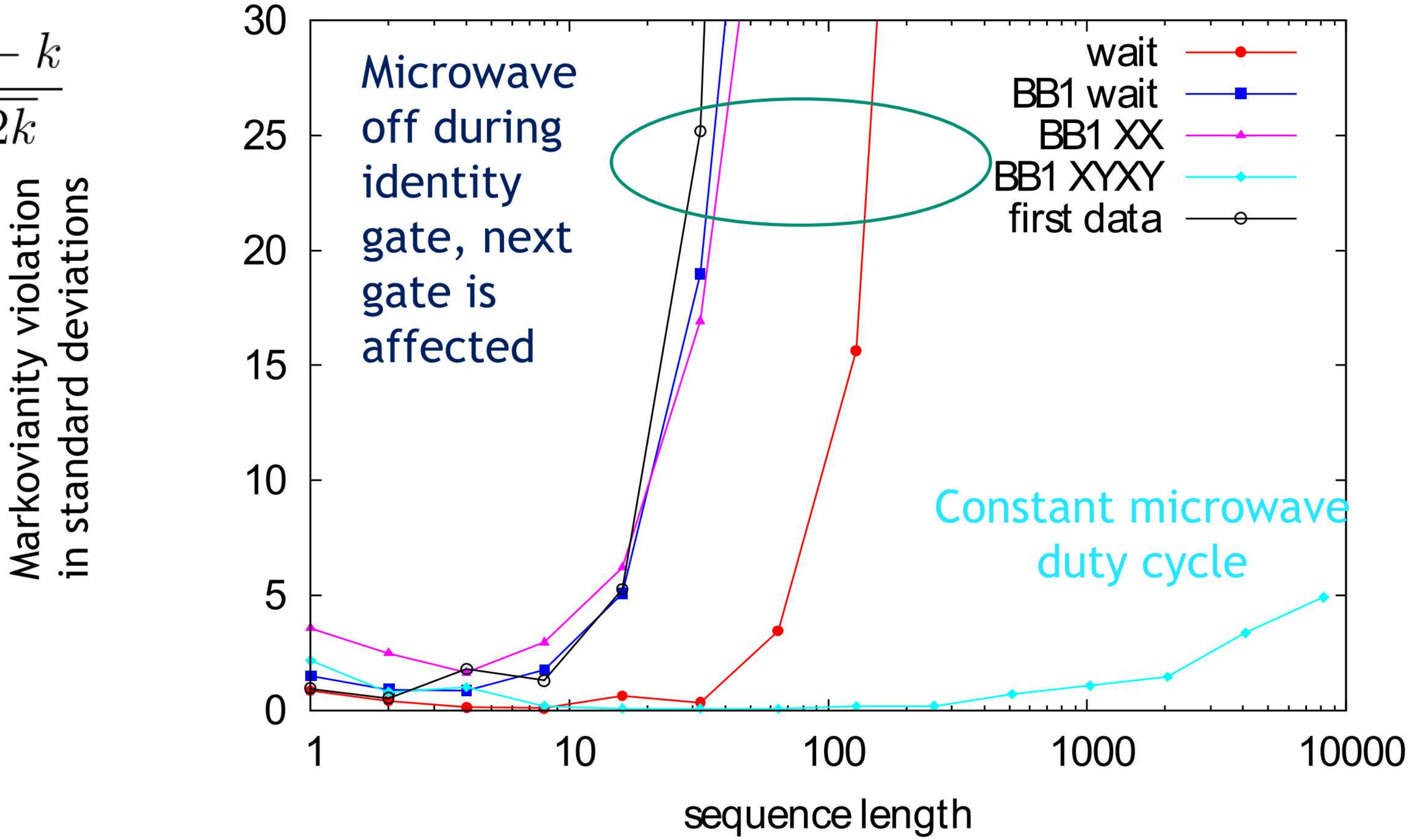

BB1 decoupled gates with decoupled identity have very small non-Markovian noise

GST model violation

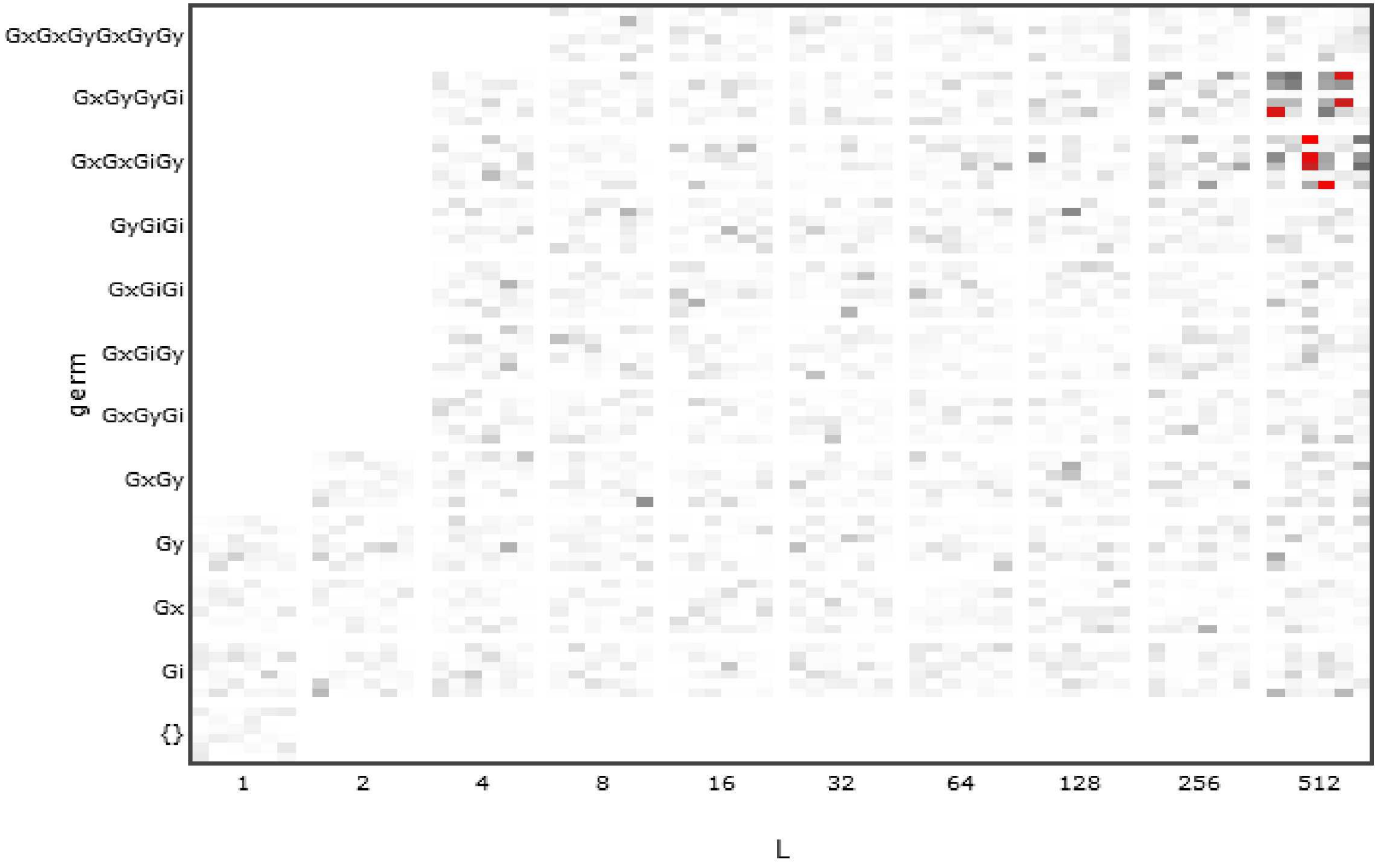

- Red boxes show sequences which violate the Markovian model
- For a Markovian realization with 95% probability there are no red boxes
- These sequences show context dependency of gates

- X- and Y- gates behave differently if applied after an I gate

- Checking and optimizing a system for

GST: Microwave results

Best results for microwave single qubit gates:

- BB1 dynamically compensated pulse sequences
- Decoupling sequence for identity gate
- Drift control for π-time and qubit frequency

95% confidence intervals

Gate	Process Infidelity	1/2 ◇-Norm
G_I	$6.9(6) \times 10^{-5}$	$7.9(7) \times 10^{-5}$
G_X	$6.1(7) \times 10^{-5}$	$7.0(15) \times 10^{-5}$
G_Y	$7.2(7) \times 10^{-5}$	$8.1(15) \times 10^{-5}$

All gates are better than the fault tolerance threshold of 9.7×10^{-5}
P. Aliferis and A. W. Cross, Phys. Rev. Lett. 98, 220502 (2007).

Two-qubit gate implementation

- Mølmer-Sørensen gates [1] using 355nm pulsed laser
- All two-qubit gates implemented using Walsh compensation pulses [2]

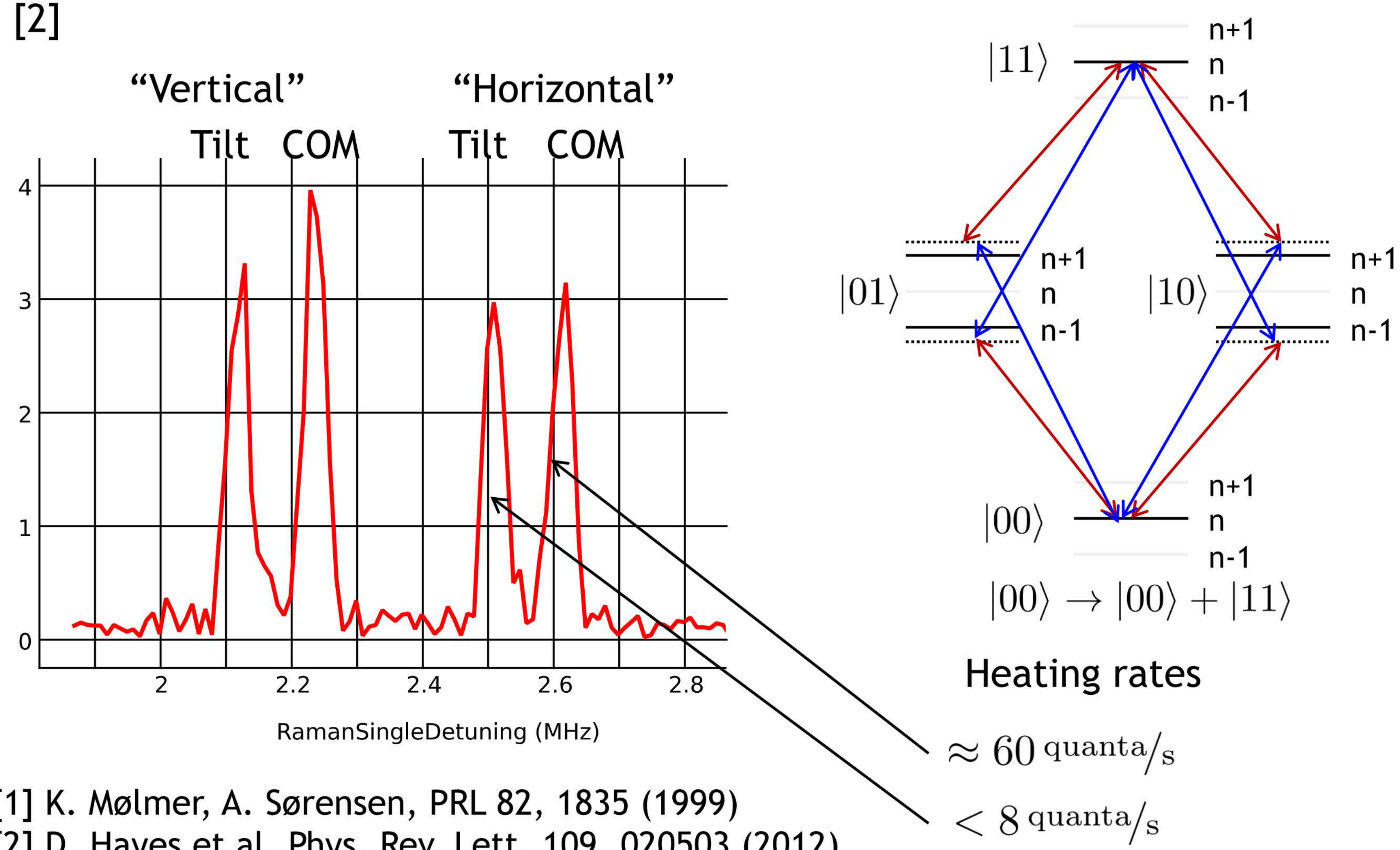

[1] K. Mølmer, A. Sørensen, PRL 82, 1835 (1999)
[2] D. Hayes et al. Phys. Rev. Lett. 109, 020503 (2012)

GST on symmetric subspace

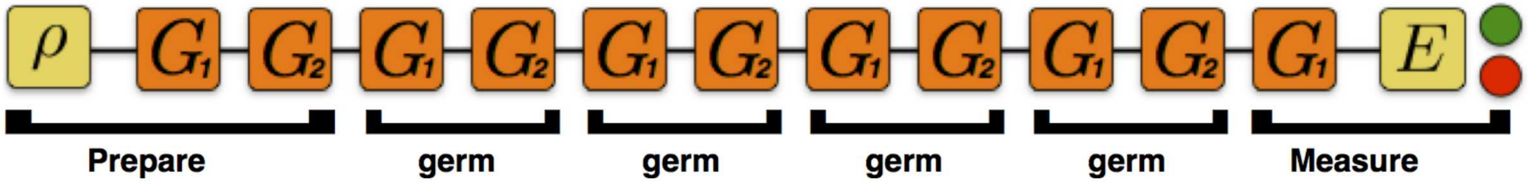

Basic gates:

G_I

$G_{XX} = G_X \otimes G_X$

$G_{YY} = G_Y \otimes G_Y$

G_{MS}

Preparation Fiducials:

$\{\}$

G_{XX}

G_{YY}

G_{MS}

$G_{XX}G_{MS}$

$G_{YY}G_{MS}$

Germs:

G_I

G_{XX}

G_{YY}

G_{MS}

$G_I G_{XX}$

$G_I G_{YY}$

$G_I G_{MS}$

$G_{XX}G_{YY}$

$G_{XX}G_{MS}$

$G_{YY}G_{MS}$

$G_I G_I G_{XX}$

$G_I G_I G_{YY}$

Detection Fiducials:

$\{\}$

G_{XX}

G_{YY}

G_{MS}

$G_{XX}G_{MS}$

$G_{YY}G_{MS}$

G_{XX}^3

G_{YY}^3

$G_{YY}^2 G_{MS}$

Two-qubit gate characterization

Gate	Process infidelity	$\frac{1}{2}$ Diamond norm
G_I	$1.6 \times 10^{-3} \pm 1.6 \times 10^{-3}$	$28 \times 10^{-3} \pm 7 \times 10^{-3}$
G_{XX}	$0.4 \times 10^{-3} \pm 1.0 \times 10^{-3}$	$27 \times 10^{-3} \pm 5 \times 10^{-3}$
G_{YY}	$0.1 \times 10^{-3} \pm 0.9 \times 10^{-3}$	$26 \times 10^{-3} \pm 4 \times 10^{-3}$
G_{MS}	$4.2 \times 10^{-3} \pm 0.6 \times 10^{-3}$	$38 \times 10^{-3} \pm 5 \times 10^{-3}$

95% confidence intervals

Process fidelity of two-qubit Mølmer-Sørensen gate > 99.5%

The best characterized two qubit gate

By the way: It’s in a scalable surface trap

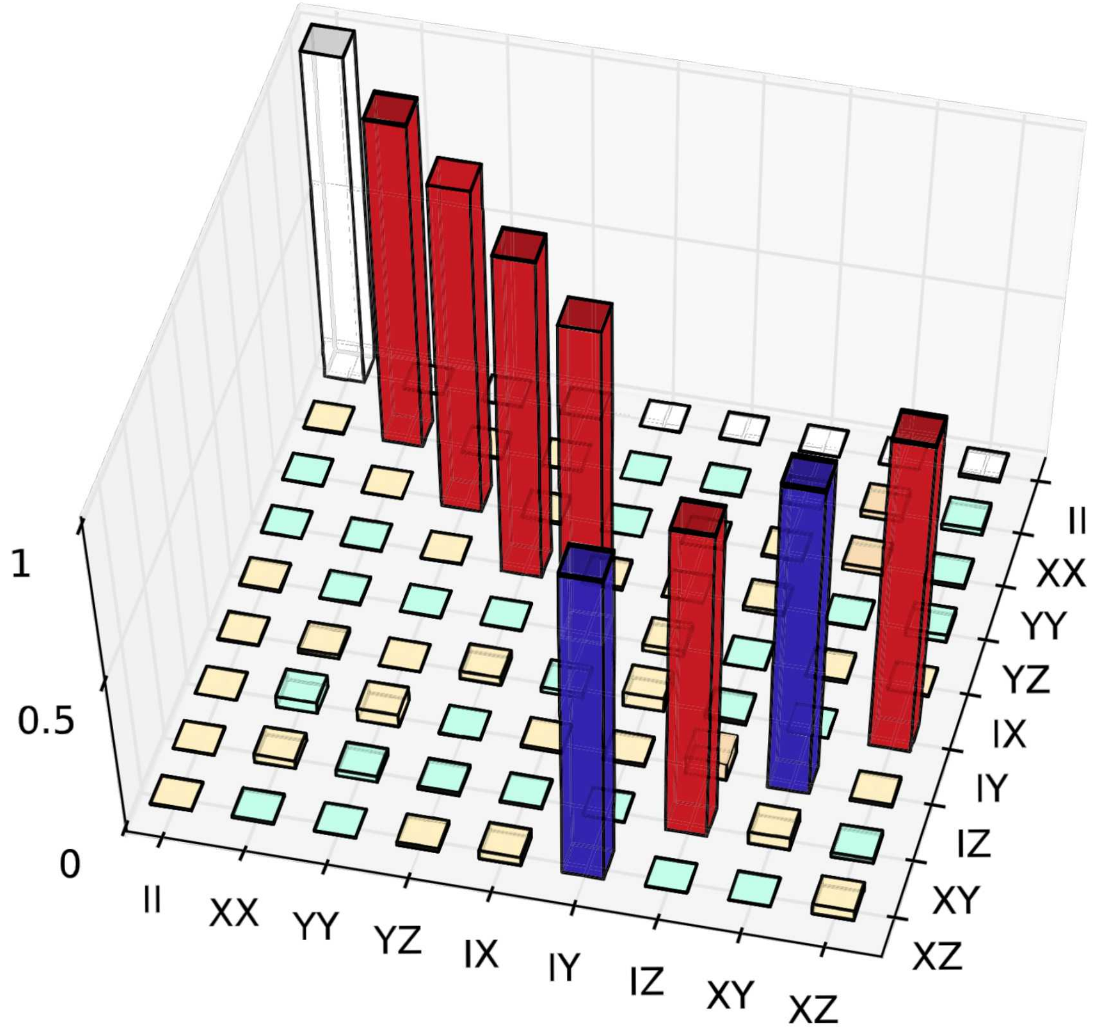

QSCOUT DOE Quantum Testbed Laboratory

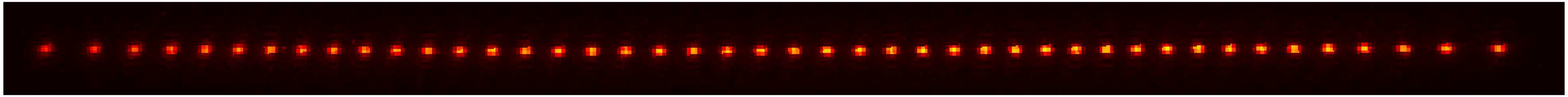

Testbed systems designed for open access to support scientific applications

- High-fidelity operations $\#gates \propto (\#qubits)^2$
- Gate-level access
- Open system with fully specified operations and hardware
- Low-level access for optimal control down to gate pulses
- Open for comparison and characterization of gate pulses
- Open for vertical integration by users

Interested? Please talk to us for access

Thanks

Trap design and fabrication

Matthew Blain
Ed Heller
Corrie Herrmann
Becky Loviza
John Rembetski
Paul Resnick
SiFab team

Trap packaging

Ray Haltli
Andrew Hollowell
Anathea Ortega
Tipp Jennings

Theory

Setso Metodi
Brandon Ruzic

Trap design and testing

Peter Maunz
Craig Hogle
Daniel Lobser
Melissa Revelle
Dan Stick
Christopher Yale

RF Engineering

Christopher Nordquist
Stefan Lepkowski